

Contribution of blowing snow sublimation to the surface mass balance of Antarctica

Srinidhi Gadde ^{1,2} and Willem Jan van de Berg ¹

¹Institute for Marine and Atmospheric Research, Utrecht University, Utrecht, The Netherlands

²Faculty of Geo-Information and Earth Observation (ITC), University of Twente, Enschede, The Netherlands

Correspondence: s.nagaradagadde@utwente.nl, w.j.vandeberg@uu.nl

Abstract. Blowing snow sublimation is an important boundary layer process in polar regions and is the major ablation term in the surface mass balance (SMB) of the Antarctic ice sheet. In this study, we update the blowing snow model in the Regional Atmospheric Climate Model (RACMO), version 2.3p3, to include, among other things, the effect of blowing snow sublimation in the prognostic equations for temperature and water vapour. These updates are necessary to remove the undesired numerical artefacts in this version's modelled blowing snow transport-fluxesflux. Specifically, instead of a uniformly discretised ice particle radius distribution used in the previous version of the model, which limited the maximum ice particle radius to $\leq 50 \mu\text{m} \leq 50 \mu\text{m}$, we use a non-uniformly discretised ice particle radii-radius distribution to include all relevant ranges-of radii-radius between 2 to 300 $\mu\text{m} \text{--} \mu\text{m}$ without any additional computational overhead. The updated model results are compared against the meteorological observations from site D47 in Adélie-Adélie Land, East Antarctica. The updates alleviate the numerical artefacts observed in the previous model results and successfully predict the power-law variation of the blowing snow fluxes-flux with wind speed while improving the prediction of the magnitude of the blowing snow fluxesflux. Furthermore, we obtain-obtained an average blowing snow layer depth of $230 \pm 116 \text{ m-m}$ at the observation site D47, which matches well-with the typical values obtained from the satellite observations. A qualitative comparison of the blowing snow frequency from updated RACMO with CALIPSO satellite observations shows that RACMO successfully predicts the blowing snow-frequency. For the period-spatial pattern of monthly blowing snow frequencies. We also compared updated RACMO results with CRYOWRF model results. While blowing snow sublimation dominates the total sublimation in RACMO, surface sublimation is the major contributor to total sublimation in CRYOWRF. Model results show that in the absence of blowing snow, sublimation in Antarctica is limited to summer months (October–March) as there is negligible surface sublimation in Antarctic winter (April–September). Introducing the blowing snow model creates an additional sublimation mechanism with its major contribution in the Antarctic winter months. For 2000 – 2010, 2012, the model-integrated blowing snow sublimation is $175 \pm 7 \text{ Gt yr}^{-1}$, an increase of 52% compared to the results of the previous model version, the contribution of integrated . The updated total sublimation, the sum of blowing snow sublimation is increased by 30%, with a yearly mean of $176 \pm 4 \text{ Gt yr}^{-1}$. It and surface sublimation, is $234 \pm 10 \text{ Gt yr}^{-1}$, which is 47% higher compared to a simulation without a blowing snow model. Increased sublimation contributes to a 1.2% reduction in the integrated SMB of the Antarctic ice sheet compared to the previous model results. In addition, we observe significant changes in the sublimation in coastal and lower escarpment zonezones, indicating the importance of the model updates to the climatology of blowing snow in Antarctica.

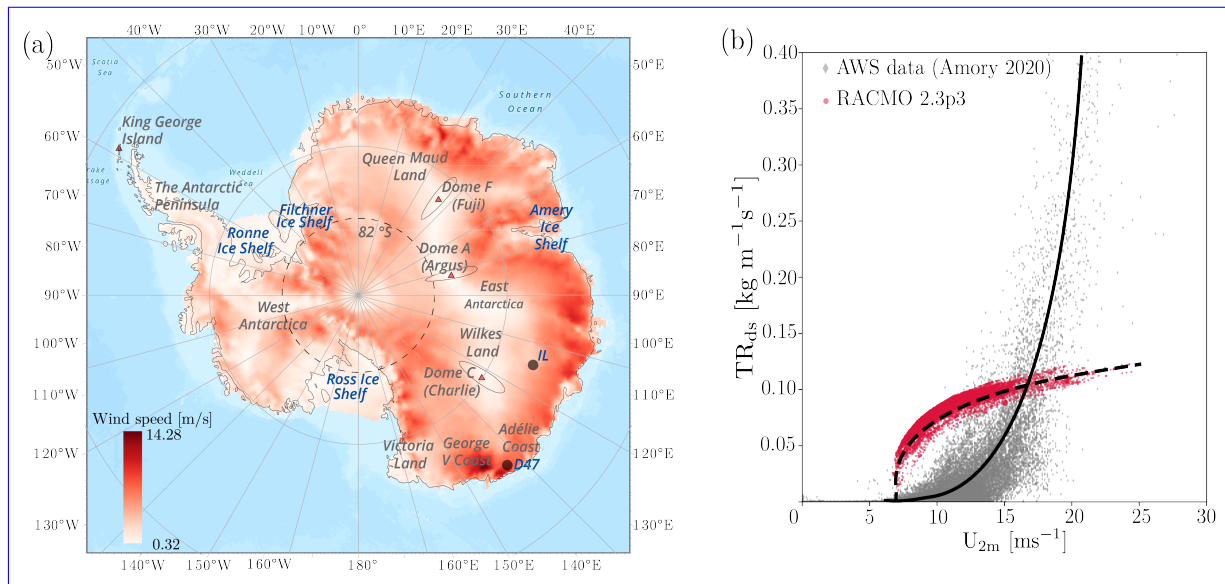


Figure 1. (a) Yearly average (2000-2012) 10-m wind speed (ms^{-1}). Location of observational site D47 in Adèle Land, East Antarctica, IL represents an interior location (71.1°S , 111.7°E), and dashed lines represent the latitude 82°S , North of which CALIPSO satellite data is available. (b) Variation of near surface blowing snow flux TR_{ds} ($\text{kg m}^{-1} \text{s}^{-1}$) vs 2-m wind speed (ms^{-1}). Solid and dashed lines represent the variation of observed and simulated (RACMO2.3p3) near-surface snow-drift fluxes, respectively. Note that RACMO2.3p3 fails to predict the variation of blowing snow transport reasonably.

1 Introduction

In the coastal regions of Antarctica, strong katabatic winds lift loose snow off the ground, causing drifting snow (e.g. Kodama et al. (1985)). When this snow rises further and is suspended in the atmospheric boundary layer, it is designated as called blowing snow. This wind-driven transport can be categorised as drifting ($< 1.8 \text{ m m a.g.l}$) and blowing ($> 1.8 \text{ m m a.g.l}$) snow (Serreze and Barry, 2005, p. 54). It redistributes the snow on the surface of an ice sheet and can also give rise to blue-ice black-ice areas, affecting the local surface energy balance (SEB) (van den Broeke and Bintanja, 1995). Furthermore, it is well known that the suspended snow particles are more prone to sublimation than surface snow (Schmidt, 1972; Bintanja, 2001). Therefore, drifting and blowing snow transport and sublimation are important factors contributing to Antarctica's surface mass balance (SMB), particularly in coastal regions (Bintanja, 1998). For brevity, from hereon, both drifting and blowing snow are combined and referred to as blowing snow.

Blowing snow is a significant contributor to the (local) SMB of the polar regions and plays a crucial role in the climate system of Antarctica. While there have been automatic weather station (AWS) observations of blowing snow-related processes from Antarctica (van den Broeke et al., 2004; Thiery et al., 2012; Barral et al., 2014; Amory, 2020), continent-wide estimates of blowing snow are difficult to obtain from observations. Continent-wide such observations. Though continent-wide estimates derived from satellite-based products are available (Palm et al., 2017). However, they are restricted to optically thin

cloud conditions and snow suspended in upper layers of the boundary layer (> 30 m a.g.l.) (Palm et al., 2011) and therefore are not suitable for estimates of near-surface blowing snow and its contribution to SMB. Hence, ~~these continent-wise~~ the continent-wide estimates can only be obtained by parameterising blowing snow processes and embedding these parameterisations in regional climate models (RCMs) (Bintanja, 1998; Déry and Yau, 2001; Lenaerts and van den Broeke, 2012; Amory et al., 2021; Toumelin et al., 2021). However, the representation of blowing snow in RCMs is challenging due to the complex and dynamic nature of ~~this~~ the phenomenon involving multiple feedbacks with related processes such as snow precipitation and surface sublimation.

Including a blowing snow model in ~~regional climate models (RCMs)~~ RCMs has been found to improve the SMB estimates in the regions where katabatic winds form (Mottram et al., 2021). Specifically, without modelling blowing snow processes, it is difficult to capture the spatial gradients in the sublimation of snow accurately (Agosta et al., 2019), which is particularly important in the escarpment regions of Antarctica. To improve our understanding of the Antarctic climate, it is crucial to accurately model the occurrence and impacts of blowing snow in RCMs. However, due to the coupled nature of blowing snow and the high sensitivity of the model to parameters, it is difficult to obtain a perfect agreement between observed and RCM estimates of blowing snow ~~fluxes~~ flux (Lenaerts et al., 2014; van Wessem et al., 2018; Amory et al., 2015, 2021).

The polar version of the regional atmospheric climate model (RACMO) (van Wessem et al., 2018; van Dalum et al., 2022) is coupled with a blowing snow scheme based on the PIEKTUK model (Déry and Yau, 2001; Lenaerts et al., 2012) to represent snow transport in polar regions. ~~Previously, in the absence of near-surface measurements of blowing snow fluxes, only blowing snow frequencies from RACMO were evaluated against the observations (Lenaerts et al., 2012). Further evaluations of RACMO against~~ Evaluation of RACMO against snow particle counter (SPC) observations from Greenland showed that RACMO2.3p1 (hereafter Rp1) overestimated the snow particle transport ~~when direct comparisons of fluxes were made (Lenaerts et al., 2014). In~~ (Lenaerts et al., 2014). ~~Therefore, in~~ RACMO2.3p2 (hereafter Rp2) (van Wessem et al., 2018), the linear saltation coefficient was subsequently halved to match ~~these blowing snow fluxes~~ the SPC observations from Greenland.

Recently, we evaluated blowing snow fluxes from ~~RACMO~~ RACMO2.3p3 (hereafter Rp3) against the SPC observational data ~~by Amory (2020)~~ at site D47 (location: 67.4°S , 138.7°E), Adélie Land, East Antarctica (Amory, 2020). Figure 1(a) shows the yearly (~~2000-2010~~ 2000-2012) average 10-m wind speed obtained by ~~RACMO~~ Rp3 and the location of the observation site D47. Since the coastal regions of Antarctica witness ~~very-high~~ very high speed winds (Fig. 1(a)) and the concentration of blowing snow particles increases with the wind speed (Radok, 1977; Budd, 1966; Amory, 2020), the blowing snow transport (TR_{ds} ~~$\text{kg m}^{-1}\text{s}^{-1}$~~ $\text{kg m}^{-1}\text{s}^{-1}$) is expected to increase in a power-law fashion with velocity. However, Figure 1(b) shows that TR_{ds} from ~~RACMO~~ Rp3 does not show a rapid increase with velocity as expected. Evaluation of ~~RACMO blowing snow fluxes~~ Rp3 blowing snow flux with observations also ~~showed that RACMO consistently underperforms in accurately predicting~~ revealed that it consistently underestimates the magnitude of the observed ~~fluxes~~ flux. The evaluation shows the need to improve the blowing snow model in ~~RACMO~~ Rp3 and systematic comparison of blowing snow fluxes against observations to obtain reliable estimates of Antarctic SMB.

In this study, several updates to the blowing snow scheme in ~~RACMO~~ Rp3 are presented. The updates aim to improve

the coupling of the blowing snow processes with [RACMO-Rp3](#) atmospheric physics. Next, near-surface blowing snow fluxes obtained from [RACMO-Rp3](#) are compared against the observed fluxes from site D47, Adélie Land, East Antarctica (Amory, 2020). The observations from site D47 are particularly suitable for evaluations since the region experiences frequent blowing snow, and the observations employ 2nd generation FlowCaptTM sensors, which have been found to predict the blowing snow fluxes with reasonable accuracy (Amory, 2020). The details of RACMO and the modifications to the blowing snow scheme in [RACMO-Rp3](#) are presented in Section 2, and details of the observational site and available data are presented in Section 3. Blowing snow frequency and fluxes from [the updated RACMO](#) are evaluated against the observations in Section 4, followed by comparing results against ~~the original version of RACMO~~ [version Rp3](#). Furthermore, we discuss the impact of the snow drift updates on the continent-wide estimates of SMB for Antarctica by comparing the modelled SMB for ~~2000-2010~~ [2000-2012 with a no-blowing snow case and model results from CRYOWRF \(Gerber et al., 2023\)](#), followed by conclusions in Section 5.

2 Model descriptions

2.1 Regional Atmospheric Climate Model (RACMO)

RACMO is built on the semi-implicit semi-Lagrangian dynamics kernel of the numerical weather prediction model HIRLAM (High-resolution limited area model; Undén et al. (2002)), version 5.0.3, with the European Center for Medium-Range Weather Forecasts (ECMWF) physics package, including both surface and atmospheric processes, from cycle 33r1 (ECMWF, 2009). The model assumes hydrostatic equilibrium, and the operational polar version (~~version 2.3p2~~, [Rp2](#)), has been verified to produce realistic results at the resolutions used in this study (van Wessem et al., 2015, 2016). This polar (p) version of RACMO2 includes a multilayer snow model that calculates the snow albedo evolution, melt, refreezing, percolation and run-off of melt-water (Greuell and Konzelmann, 1994; Ettema et al., 2010; Kuipers Munneke et al., 2011). It also includes a blowing snow scheme based on the PIEKTUK model (Déry and Yau, 1999; Lenaerts et al., 2012).

In the newer version of [RACMO2, version 2.3p3](#), ~~hereafter abbreviated as~~ [Rp3](#), the snow and ice albedo parameterisations were updated using Two-streAm Radiative ~~Trasnfer~~ [TransfEr](#) in Snow model (TARTES; Libois et al. (2013)) coupled with the Spectral-to-NarROWBand ALbedo (SNOWBAL) module, version 1.2 (van Dalum et al., 2019). [Rp3](#) has produced results that compare well with both in-situ and remote sensing observations of SMB of Antarctica (van Dalum et al., 2022). [RACMO2 Rp2](#) and [Rp3](#) are introduced in detail in Noël et al. (2018) and van Dalum et al. (2019), respectively. At the lateral boundaries, the simulations presented here are forced with ECMWF ERA5 reanalysis data (Hersbach et al., 2020) with an update interval of 3 hours.

2.2 Blowing snow model

In [RACMO-Rp3](#), we use the bulk (non-spectral) version of the PIEKTUK model (Déry and Yau, 1999), which employs an evolution equation for the mixing ratio of blowing snow q_b (kg kg^{-1}) ~~q_b (kg kg^{-1})~~ and an additional equation for the evolution of snow particle number concentration N , which is the double-moment version of the ~~PIEKTUK model~~ [\(model hereafter](#)

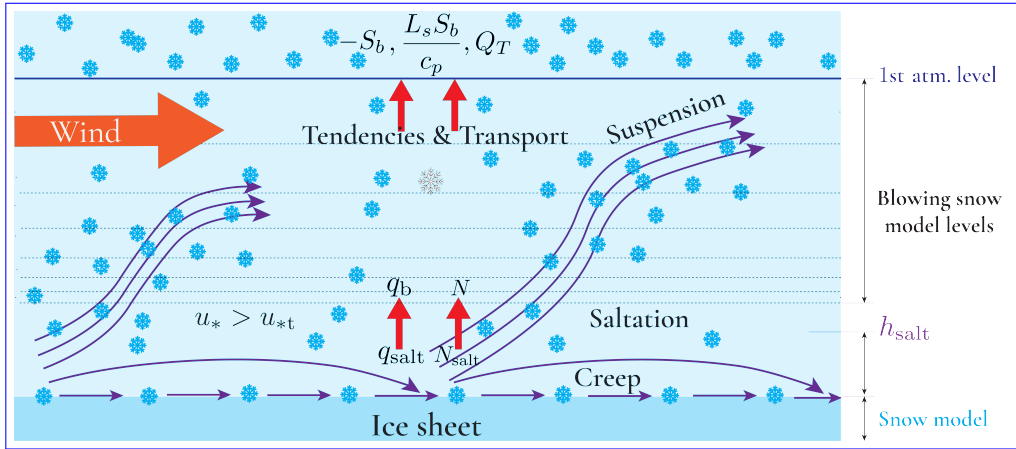


Figure 2. Schematic showing the blowing snow model levels, Rp3 model levels, and key processes involving blowing snow. Q_T represents the snow transport due to blowing snow. The figure shows that the model level of blowing snow is above the saltation height. In the schematic, q_b (mixing ratio) and N (number concentration) represent the boundary conditions for the blowing snow model calculated from q_{salt} and N_{salt} using the classical equation for suspended particle concentration.

PIEKTUK-D, Déry and Yau (2001)). ~~PIEKTUK is an Inuktitut word for blowing snow (Déry et al., 1998).~~ Here, we introduce only the essential features of the PIEKTUK model, and the additional details can be found in Déry and Yau (2001).

110 PIEKTUK is an Inuktitut word for blowing snow (Déry et al., 1998). Figure 2 shows the blowing snow processes and the coupling between ~~PIEKTUK and RACMO~~ PIEKTUK-D and Rp3, presenting the important snow transport mechanisms over an ice sheet. When the friction velocity, a measure of the wind shear at the surface, exceeds the threshold friction velocity, the snow particles perform a downwind motion of a series of jumps or skips, a process called saltation. When the saltating snow particles get suspended in the boundary layer due to turbulent mixing, they form the blowing snow. In ~~PIEKTUK~~ PIEKTUK-D,
 115 this transition from saltation to suspension, governed by different physical mechanisms, is assumed to happen at the elevation h_{salt} . ~~It is worth mentioning here that, in RACMO, the suspension is coupled with saltation, as saltation does not contribute to long-distance snow transport; the model is only activated when the wind is energetic enough to facilitate suspension. For the blowing snow governing equations, the saltation flux parameterisation serves the boundary condition. In Section ?? we introduce the saltation flux parameterisation followed by the evolution equations of blowing snow in Section ??.~~

120 2.2.1 Saltation flux

To calculate the sublimation and transport of blowing snow, the evolution equation for the blowing snow mixing ratio q_b (kg kg^{-1}) is written as:

$$\frac{\partial q_b}{\partial t} = \frac{\partial}{\partial z} \left(K_b \frac{\partial q_b}{\partial z} + v_b q_b \right) + S_b \quad (1)$$

125 where t (s) denotes time, z (m) the vertical coordinate, v_b (m s^{-1}) is the bulk terminal velocity, K_b ($\text{m}^2 \text{s}^{-1}$) represents turbulent eddy diffusivity for blowing snow, and S_b ($\text{kg kg}^{-1} \text{s}^{-1}$) the bulk sublimation rate. The lowest blowing snow model level is set to 0.1 m, at the top of the saltation layer at height h_{salt} . The boundary condition for solving Eq. (1) is given by relating the blowing snow mixing ratio q_b at the lowest model level with the mixing ratio at the top of the saltation layer, q_{salt} . There exist several empirical formulations for erosion of the snow particles in the saltation layer, q_{salt} (kg kg^{-1}). In previous RACMO versions, it has been q_{salt} (kg kg^{-1}). In Rp1, saltation flux was parameterised using Déry and Yau (1999),

$$130 \quad q_{\text{salt}} = c_{\text{salt}} \left(\frac{1 - (u_1 - u_{\text{thr}}/U_{\text{fml}})^{2.59}}{2.59} \right)^{2.59} / u_*, \quad (2)$$

in which c_{salt} is a constant, initially set to 0.385 and returned to 0.192 in RACMO versions 2.3p2-Rp2 and Rp3, respectively. Furthermore, u_{thr} represents the threshold wind velocity (m s^{-1}), and U_{fml} represents wind speed at the first model level (m s^{-1}). The threshold wind velocity is defined by $u_{\text{thr}} = 9.43 + 0.18 T_{2\text{m}} + 0.0033 T_{2\text{m}}^2$ with $T_{2\text{m}}$ in $^{\circ}\text{C}$ (Déry and Yau, 1999).

135 In this study Rp3, we update the saltation parameterisation with an alternative empirical parameterisation, proposed by Pomeroy (1989), is Pomeroy (1989),

$$q_{\text{salt}} = \frac{e_{\text{salt}}}{gh_{\text{salt}}} \frac{e_{\text{salt}}}{gh_{\text{salt}}} \left(u_*^2 - u_{*t}^2 \right), \quad (3)$$

140 where e_{salt} , the saltation efficiency, is set to $1/(3.25u_*)$, u_* (m s^{-1}) is the friction velocity, $h_{\text{salt}} = 0.08436u_*^{1.27}$ represents the thickness of the saltation layer (m) according to the relation of Pomeroy and Male (1992), $g = 9.81$ is the gravitational acceleration (m s^{-2}), and u_{*t} represents the threshold friction velocity (m s^{-1}). Schematic showing the blowing snow model levels, RACMO model levels, and key processes involving blowing snow. Q_T represents the snow transport due to blowing snow. The figure shows that the model level of blowing snow is above the saltation height. In the schematic, q_b (mixing ratio) and N (number concentration) represent the boundary conditions for the blowing snow model calculated from q_{salt} and N_{salt} using the classical equation for suspended particle concentration. The parameterisation of the threshold friction velocity in Equation Eq. (3) is given by Gallée et al. (2001):

$$145 \quad u_{*t} = u_{*t0} \exp \left(\frac{-n}{1-n} + \frac{n_0}{1-n_0} \right), \quad (4)$$

where, $n = (1 - \rho_s/\rho_i)$, $n_0 = (1 - \rho_0/\rho_i)$, with ρ_s as the actual mean snow density of the upper 5 cm, and ρ_i is the density of ice. n_0 is the porosity of fresh snow with $\rho_0 = 300 \text{ kg m}^{-3}$. The reference threshold friction velocity u_{*t0} is calculated based on the potential for snow erosion by the wind, which u_{*t0} is characterised by a snow mobility index, Mo , which is given by the relation, $Mo = 0.75d - 0.5s + 0.5$, $Mo = 0.75d - 0.5s + 0.5$, where the variables d and s represent the snow grain dendricity, and sphericity, respectively. However, dendricity and sphericity are not modelled in RACMO. Therefore, we take $d = s = 0.5$, hence set Mo to 0.625. Finally, u_{*t0} The threshold friction velocity based on (Gallée et al., 2001), depend on the snow mobility index which denotes the potential for snow erosion by the wind, with $Mo = 0.75d - 0.5s + 0.5$, where d and s represent dendricity and sphericity

155 of fresh snow. Gallée et al. (2001) mention that the crystal shape of freshly fallen snow does not allow a large grain cohesion in the snowpack. Therefore, this allows relatively high snow mobility index Mo values for large d . Sintering is enhanced when the number of rounded shapes increases so that Mo decreases when s decreases. Explicitly modelling the snow mobility index requires solving prognostic equations for snow particle characteristics. Without sophisticated models for snow particle characteristics, the snow mobility index was set to 0.625 ($d = 0.5$ and $s = 0.5$) to match blowing snow frequency observations. A
 160 detailed discussion is available in Lenaerts et al. (2012). A parametric study of the snow particle characteristics is out of the scope of the present study.

Finally, u_{*t0} is defined by Gallée et al. (2001) as

$$u_{*t0} = \frac{\log(2.868) - \log(1 + Mo)}{0.085} \frac{\log(2.868) - \log(1 + Mo)}{0.085} C_D^{0.5}, \quad (5)$$

where $C_D = u_*^2 / U_{fml}^2$ represents the drag coefficient of momentum.

165 2.2.1 Evolution of blowing snow

To calculate the sublimation and transport of blowing snow, the evolution

The governing equation for the blowing snow mixing ratio q_b (kg kg^{-1}) is written as:

$$\frac{\partial q_b}{\partial t} = \frac{\partial}{\partial z} \left(K_b \frac{\partial q_b}{\partial z} + v_b q_b \right) + S_b$$

where t (s) denotes time, z (m) the vertical coordinate, v_b (m s^{-1}) is the bulk terminal velocity, K_b ($\text{m}^2 \text{s}^{-1}$) represents turbulent eddy diffusivity for blowing snow, and S_b ($\text{kg kg}^{-1} \text{s}^{-1}$) the bulk sublimation rate. This equation is implicitly discretised in
 170 the vertical direction and solved using the tri-diagonal matrix algorithm. The lowest blowing snow model level is set to 0.1 m — at the top of the saltation layer at height h_{salt} — and the boundary condition for solving Equation (1) is given by relating the blowing snow mixing ratio q_b at the lowest model level with the mixing ratio at the top of the saltation layer, q_{salt} (Eq. (2) in RACMO2 or Eq. (3) in the updated version) (Déry and Yau, 1999).

175 RACMO employs the double-moment PIEKTUK model. Therefore, an additional equation is employed to obtain the evolution the concentration of particles (N) is

$$\frac{\partial N}{\partial t} = \frac{\partial}{\partial z} \left(K_N \frac{\partial N}{\partial z} + v_b N \right) + S_N. \quad (6)$$

Here, K_N ($\text{m}^2 \text{s}^{-2} \text{m}^2 \text{s}^{-2}$) is the eddy diffusivity for N , and S_N ($\text{m}^3 \text{s}^{-1} \text{m}^3 \text{s}^{-1}$) denotes the rate of change of particle numbers due to the sublimation process. The lower boundary condition for solving Equation Eq. (6) is here also the particle concentration
 180 at the top of the saltation layer (N_{salt}) (Déry and Yau, 1999), which will be defined below.

In PIEKTUK-D model, the bulk blowing snow mixing ratio q_b is related to N via the spectral number density $F(r)$, following Schmidt (1982):

$$q_b = \frac{4\pi\rho_{ice}}{3\rho} \int_0^\infty r^3 F(r) \underline{d}r, \quad (7)$$

where the distribution of $F(r)$ follows two-parameter gamma distribution (Budd, 1966; Schmidt, 1982) by the relation:

$$185 \quad F(r) = \frac{Nr^{(\alpha-1)} \exp^{-r/\beta}}{\beta^\alpha \Gamma(\alpha)}, \quad (8)$$

where, r represents the radius of ice particles, α (dimensionless) and β (mm) the shape and scale parameters of the gamma distribution Γ . ~~Substituting Equation~~ ~~Substituting, Eq.~~ (8) in (7), we obtain the particle number concentration N_{salt} at the saltation layer:

$$N_{\text{salt}} = \frac{3\rho q_{\text{salt}}\Gamma(\alpha)}{4\pi\rho_{\text{ice}}\Gamma(\alpha+3)\beta^3}, \quad (9)$$

190 with $\alpha = 4.0$, $\beta = 100/\alpha$ (~~mm~~ μm), and density of ice $\rho_{\text{ice}} = 917 \text{ kg m}^{-3}$. ~~Equation~~ ~~kg m~~ ~~Eq.~~ (7) is discretised with the hypothesis that ice particle size follows a two-parameter gamma distribution, with particle size bins covering particles of radius 2 to ~~300 mm~~ ~~300~~ μm (Déry et al., 1998).

Finally, in the blowing snow model in ~~RACMO~~, the mass change of an ice particle due to the blowing snow sublimation is given by the model of Thorpe and Mason (1966):

$$195 \quad \frac{dm}{dt} = \left(2\pi r \sigma - \frac{Q_r}{K N_{\text{Nu}} T_a} \left[\frac{L_s}{R_v T_a} - 1 \right] \right) / \left(\frac{L_s}{K N_{\text{Nu}} T_a} \left[\frac{L_s}{R_v T_a} - 1 \right] + R_v \frac{T_a}{N_{\text{Sh}} D e_i} \right), \quad (10)$$

where σ (dimensionless and negative) is the water vapour deficit with respect to ice $(e - e_i)/e_i$, where e and e_i are the vapour pressure and its value at saturation over ice. T_a is the ambient air temperature (K), K the thermal conductivity of air (~~W m~~ ~~K~~ ~~W m~~ ~~K~~), L_s the latent heat of sublimation (~~J kg~~ ~~K~~ ~~J kg~~ ~~K~~), R_v the gas constant for water vapour, and D the molecular diffusivity of water vapour in air (~~m~~ ~~s~~ ~~m~~ ~~s~~), Q_r the net radiation transferred to the ice particle (~~W~~), and N_{Nu} and N_{Sh} being the Nusselt and Sherwood numbers.

2.3 Major changes to blowing snow model in RACMO

Six major updates in the implementation of ~~PIEKTUK in RACMO~~ ~~PIEKTUK-D in Rp3~~ are summarised below :

1. In ~~RACMO~~ ~~Rp3~~, uniformly discretised 12-particle size bins were used, with a constant particle bin size ~~$\Delta r = 4 \mu\text{m}$~~ ~~$\Delta r = 4 \mu\text{m}$~~ . Therefore, size bins with a mean particle radius greater than ~~50 mm~~ ~~50~~ μm were excluded, which caused the unexpected variation of TR_{ds} observed in Fig. 1(b). ~~Limited ice particle radius classes influenced the calculation of the bulk terminal velocity and the boundary conditions for Equations (6) and (1).~~ To solve the issue, we use a grid stretching technique similar to ~~DNS~~ ~~Direct Numerical Simulations (DNS)~~ of channel flows to obtain non-uniform ~~grids~~ ~~distribution~~ with smooth stretching ~~following a tangent hyperbolic function~~ (Vinokur, 1983). We now use ~~non-uniform discretisation with~~ 16-particle size bins with varying Δr to include all relevant particle size classes with particles of mean radius for each bin from 2 to ~~300 mm~~ ~~300~~ μm , while keeping the computational overhead the same as before. ~~Increase in the Δr is non-uniform and follows a tangent hyperbolic function similar to the stretched grids used in DNS of channel flow.~~ Déry et al. (1998) report convincing results by including particles of mean radius for each bin from 2 to ~~254 mm~~ ~~254~~ μm .

2. Previously, in the ~~PIEKTUK model in RACMO~~ blowing snow model of Rp3, 32 vertical levels equidistant on a logarithmic scale were used. ~~However, the vertical levels were not at the same height as the RACMO model levels, which made it difficult to include the blowing snow quantities as tendencies in the prognostic equations of water vapour and temperature. Furthermore, the blowing snow~~ The blowing snow model was not fully coupled to the boundary-layer model ~~in RACMO~~ as the blowing snow grid levels did not match the model atmospheric levels. Specifically, ~~in the previous model version,~~ instead of the ~~simulated velocity profile from RACMO, log-law-based velocity and temperature profiles were extrapolated from wind velocity and temperature at the first RACMO model~~ actual velocity profiles, temperature and velocity profiles were reconstructed using logarithmic relations from the first model atmospheric level. In addition, the friction velocity (u_*) was recalculated in the blowing-snow model, assuming near-neutral conditions. These inconsistencies have now been resolved, and actual velocity and temperature profiles and friction velocities from the ~~RACMO boundary-layer~~ boundary layer model are used, which ~~constitutes~~ constitutes another major improvement. We have reduced the vertical levels to 16 to reduce computational expenses, with ~~8~~ eight logarithmically varying levels up to the lowest ~~RACMO~~ model level (dashed lines in Figure 2). ~~The first model level is set to 0.1 m, which is assumed to be the top of the saltation layer (h_{salt}).~~ Furthermore, above the lowest ~~RACMO model~~ atmospheric level, the ~~PIEKTUK model~~ PIEKTUK-D model levels coincide with the ~~RACMO model~~ model atmospheric levels, and this facilitates easier coupling of blowing snow sublimation as tendencies in the prognostic equations.
3. We found that ~~the PIEKTUK model~~ PIEKTUK-D, when coupled ~~with RACMO, is also to Rp3, is~~ highly sensitive to the model time step. ~~In PIEKTUK-D, the integrated blowing snow flux quickly reaches equilibrium, and it depends on the time step used to solve the evolution equations.~~ While Déry and Yau (1999) specify a model time step of 2 seconds for ~~PIEKTUK-B; in RACMO~~ PIEKTUK-D; in Rp3, the model time step was of the order of 300 – 600 seconds. This time step was too large to predict the drift fluxes reliably. To overcome this, we introduce sub-stepping in the blowing snow model. ~~By performing sensitivity analysis, we found that a constant time step of~~ We ran the model with different Δt , with different time step sizes. We found large difference between the values of integrated blowing snow flux for $\Delta t = 600, 300, 100, 50, 20, 10$ seconds produces reliable estimates. ~~and 5 seconds. For $\Delta t = 10$ and $\Delta t = 5$, the magnitude of blowing snow flux was nearly the same, so we choose $\Delta t = 10$ s.~~ Furthermore, the model quickly reaches a steady state in 5 sub-steps. Therefore, we use five sub-steps with a time step of 10 seconds and the fluxes from the last sub-step are taken as the representative flux for the ~~whole RACMO full Rp3~~ model step.
4. In the original PIEKTUK model implementation by Déry and Yau (1999), the blowing snow mixing ratios are reset to zero only if the friction velocity is lower than the threshold friction velocity in two consecutive time steps, providing a realistic initial approximation of blowing snow quantities in each time step. However, previously in ~~RACMO~~ Rp3, N and q_b were reset to zero after every model time step, though in reality, the blowing snow events last for hours. Resetting the flux to zero is unrealistic and calls for a proper initialisation of the variables. Therefore, we now initialise N and q_b from the previous time step if two consecutive time steps satisfy the condition $u_* > u_{*t}$; otherwise, the values are reset to zero, indicating the end of the blowing snow event.

5. In ~~RACMO~~In Rp3, the bulk sublimation rate S_b was used to calculate an integrated blowing snow sublimation flux, and this integrated moisture flux was added to the surface. While this approach works reasonably in obtaining SMB estimates, it is ~~only partially physical not realistic~~ since it limits the effect of blowing snow sublimation to the surface. To rectify this error in representation, we now add blowing snow sublimation rate ($-S_b$) and latent heat due to blowing snow ($L_s S_b / c_p$) as tendencies to the prognostic equations of atmospheric water vapour and temperature, respectively. ~~For the PIEKTUK model levels below the lowest RACMO model level, a height-averaged tendency is calculated. It is used as the representative value for that RACMO level, and no moisture flux was added at the surface. For the rest of the RACMO model levels, the tendencies are obtained directly from the corresponding PIEKTUK vertical levels.~~
6. In ~~RACMO~~Rp3, snowdrift was modelled if $u_* > u_{*t}$ and ~~Equation Eq.~~ (2) was used to estimate the saltation flux. This parameterisation caused sharp variations in the saltation flux in ~~RACMO~~Rp3 and was not optimal. Therefore, the saltation flux is now derived with ~~Equation Eq.~~ (3), which produces smooth variations of q_{salt} . Furthermore, ~~Equation Eq.~~ (3) is ~~widely used in literature. also used in the MAR model to parameterise saltation flux (Amory et al., 2021).~~ Finally, the formula to derive the vapour saturation pressure to ice (e_i) in ~~Equation Eq.~~ (10) has been updated to the AERKi formula (Alduchov and Eskridge, 1996; CY45R1—Part IV, 2018), as this formula is used in IFS code in which the blowing snow module is embedded.

3 ~~Observation site and data~~Datasets for model evaluation

~~The~~

3.1 In situ snowdrift observations

~~The in situ observations used for evaluation are presented and discussed in detail by Amory (2020) and Amory et al. (2020a); here, we summarise the key information.~~ The observational site D47 (location: 67.4°S, 138.7°E, Fig. 1(a)), is located at an elevation of 1560 mm, and at a distance of 105 km from the shore (~~Amory, 2020~~). Due to its topographical situation, the site experiences strong katabatic winds with a strong directional consistency (~~Amory (2020)~~). Due to the high surface winds, the site experiences frequent blowing snow events (~~Amory, 2020~~) and is ideally suited for evaluating RACMO results. For evaluation, observations of near-surface quantities such as 2-m wind speed, temperature, and air relative humidity are used, complemented with half-hourly drifting-snow transport fluxes. These observations are available for ~~the years~~ 2010–2012 with half-hourly temporal resolution. The drifting-snow transport fluxes are measured with second-generation FlowCapt™ sensors. The sensors convert the acoustic vibration caused by blowing snow particles into integrated snow mass flux. The equipment consists of two 1-m length acoustic tubes, superimposed vertically to measure snow flux in the first 2 m above the ground. ~~A detailed setup and observational site description can be found in Amory (2020) and Amory et al. (2020a).~~

The blowing snow scheme in ~~RACMO~~Rp3 has multiple levels, with the lowest vertical level set at 0.1 mm. For comparison with observations, we obtain an average, vertically integrated, blowing snow flux, $Q_{T,RACMO}$ (~~kg m⁻² s⁻¹~~kg m⁻² s⁻¹), from the lowest model level ~~upto up to~~ 2-m height. Following Amory et al. (2021), since there are two acoustic tubes for measurement,

we combine snow mass flux from both the tubes into an average, near-surface, mass flux $Q_{T,OBS}$ ($\text{kg m}^{-2} \text{s}^{-1}$), as :

$$280 \quad Q_{T,OBS} = \frac{Q_{T,1}h_1 + Q_{T,2}h_2}{h_1 + h_2} \frac{Q_{T,1}h_1 + Q_{T,2}h_2}{h_1 + h_2}, \quad (11)$$

where, $Q_{T,1}$ is the observed snow mass flux integrated over the exposed length of h_1 of the corresponding 2G-FlowCapt™ sensor. ~~Furthermore, at site D47, wind speeds are available from the mast at a 2-meter height.~~ The height of the sensor at D47 is 2.8 m. However, Amory (2020) mention that, due to harsh weather conditions at D47, it was difficult to reset the height of the sensors owing to the elevation changes due to snow. As a result, by late December 2012, the measurement heights decreased from their initial values to 1.5 m for wind speed and direction and 0.9 m for temperature and relative humidity. Therefore, we compare the instantaneous fluxes for the year 2011. The data is made available on Zenodo as quantities at 2-m height. Since the first atmospheric level in RACMO (approximately 8–10 m) is above this height, we obtain the 2-m wind speed using the Monin-Obukhov similarity theory.

3.2 Satellite data for evaluating monthly blowing snow frequency

290 We compare model results with lidar data from CALIPSO (Cloud-Aerosol Lidar and Infrared Pathfinder Satellite Observation, Palm et al. (2017)), which measures blowing snow quantities for the Antarctic Ice Sheet north of 82 °S (Palm et al., 2017, 2018). These satellite observations include only those blowing snow layers deeper than 30 m and only those events without clouds. Making an accurate one-to-one comparison of the model results with the satellite observations requires filtering of the model results to layers deeper than 30 m and for cases with no or optically thin cloud conditions, of which the former is not possible with the data exported from the current RACMO simulations. Therefore, we use the satellite observations to look at the seasonal patterns and only qualitatively compare the model results.

4 Results and discussion

Three ~~RACMO-Rp3~~ simulations for 2000–2012, forced by ERA5 reanalysis data, were run for the evaluation presented here. The first one, hereon referred to as RpNew, employed all updates listed in Section 2.3. A second simulation was carried out with the blowing snow scheme switched off, hereon referred to as NO-DRIFT, to study the effects of blowing snow compared to the no-blowing snow scenario. Finally, a simulation with the original blowing snow code of ~~RACMO2.3p3, hereafter referred to as Rp3~~, has been carried out to compare the change in SMB estimates and related quantities. ~~This simulation was needed as the simulation presented by van Dalum et al. (2019) lacked the detailed blowing snow output needed for the study presented here.~~

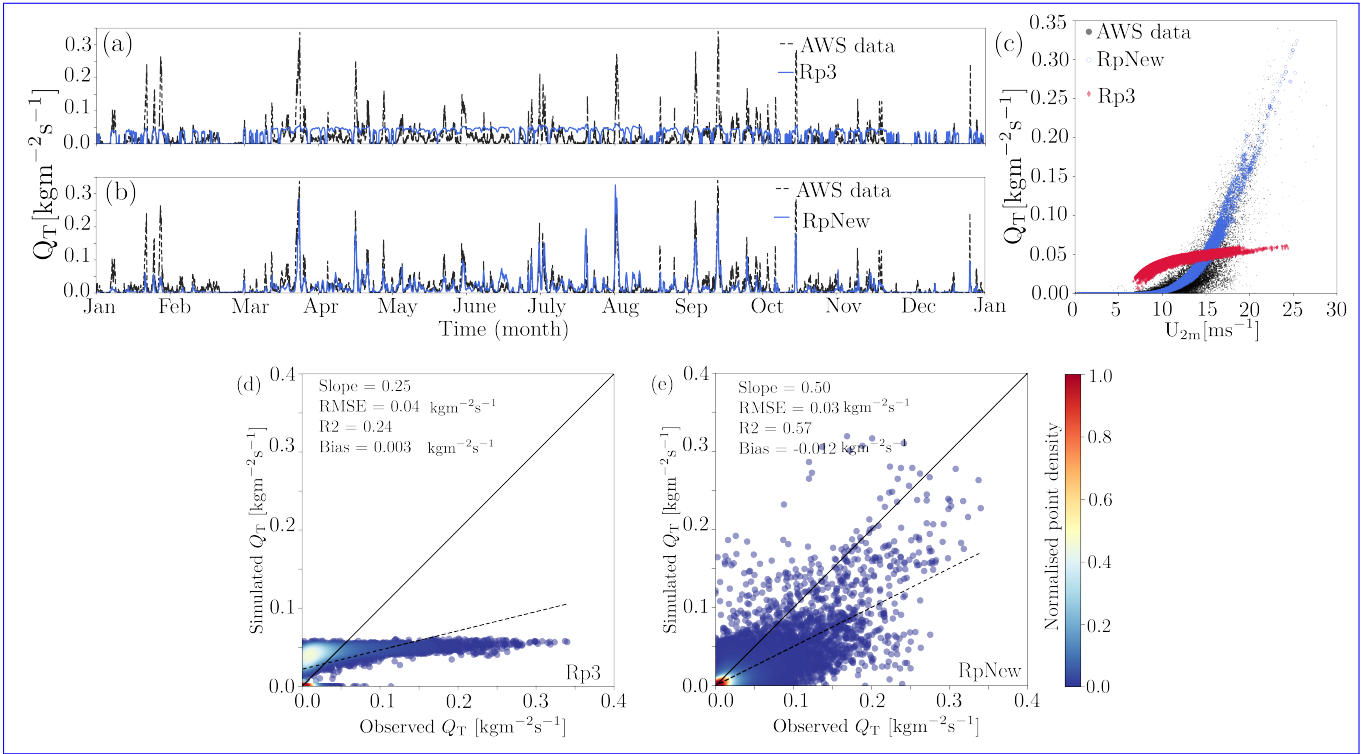


Figure 3. Comparison of simulated instantaneous near-surface blowing snow flux Q_T ($\text{kgm}^{-2}\text{s}^{-1}$) with observations for the year 2011: (a) Rp3, (b) RpNew (c) Variation of near-surface blowing snow flux Q_T with 2-m wind speed U_{2m} (ms^{-1}). Open circular, filled red diamond, and filled circular markers represent data from RpNew, Rp3, and AWS data, respectively. Observed and simulated blowing snow fluxes $\text{kgm}^{-2}\text{s}^{-1}$ (d) Rp3, and (e) RpNew. Solid lines represent the 1:1 line and the dashed lines represent the best-fit line. The colours represent the normalised point density from low (0.0, black) to high (1.0, red).

305 4.1 Model evaluation with observations at site D47

4.1.1 Blowing snow flux and near-surface relative humidity

Figure 3(a) presents the instantaneous blowing snow mass flux obtained from Rp3 compared with the observations for the year 2011. It is evident from the figure that Rp3 does not reliably predict the magnitude of the blowing snow. In Rp3, the linear saltation coefficient c_{salt} (Eq. (2)) was reduced (van Wessem et al., 2018) which resulted in the low, limited snow transport flux seen in Figure 3(a). As halving c_{salt} roughly led to halving the snow drift flux, the RACMO versions preceding version 2.3p2, with doubled c_{salt} , overestimated Q_T for most of the time (not shown).

Figure 3(b) presents the instantaneous blowing snow mass flux obtained with the RpNew. We observe that RpNew works well in predicting the magnitude of the blowing snow flux. Specifically, the magnitude of the blowing snow flux matches the observations reasonably well in the Antarctic winter (April–September). However, it is underestimated in the Antarctic summer (October–March). The underestimation might be related to the amount of loose snow available at the surface, possibly due

315

to inaccuracies of the modelled surface snow compaction in summer or the direct interaction between precipitation and snow drift, which Rp3 does not resolve. As we found no clear cause for the underestimation of snow drift during summer, further study is necessary to uncover the seasonal differences in the blowing snow flux.

Figure 3(c) presents the variation of blowing snow mass flux with the near-surface wind speed. Flux from Rp3 fails to
320 produce power-law variation with the wind speed; however, RpNew successfully predicts it. The primary reason for this improvement is the non-uniform ice particle radius distribution, allowing us to include all relevant ice particles in the range between 2 to 300 μm . Coupled with the better coupling with RACMO prognostic variables and sub-stepping, the behaviour of the flux follows the expected power-law variation seen in Figure 3(c).

In Figure 3(d) and (e), we present the comparison of simulated near-surface blowing snow mass flux with observed flux for
325 Rp3 and RpNew, respectively. Simulated flux from Rp3 has a positive bias, with a very low R^2 (p-value < 0.01) indicating that Rp3 fails to capture the variability in the blowing snow flux observations. The predictions with Rp3 also have a higher RMSE of $0.035 \text{ kg m}^{-2} \text{ s}^{-1}$. Also, it is apparent from Figure 3(d) that Rp3 fails to predict the blowing snow fluxes reliably when compared with the observations. In contrast, with RpNew, we have a reasonable agreement between the observed and simulated fluxes (Fig. 3(e)) with $R^2 = 0.56$ (p-value < 0.01). The agreement indicates that the changes introduced significantly improve
330 its ability to predict the blowing snow fluxes. Though the predictions are considerably improved compared to the observations, both Rp3 and RpNew underestimate the blowing snow fluxes. The underestimation is mostly due to the underestimation of velocities reported in Table A1 and the model sensitivity to the chosen parameters. Since the snow transport flux varies in a power-law fashion with the wind speed (Radok, 1977; Budd, 1966; Amory, 2020), the flux is highly sensitive to the wind-speed predictions; even a slight underestimation in the velocity introduces a significant difference in the blowing snow mass flux.

Though RpNew results show the desired behaviour, it fails to capture the spread in the observational data (Fig. 3(c)). Through
335 sensitivity analysis of the data, we found that the spread in the data depends on the modelling choices made, e.g. the parameter α in two-parameter gamma distribution (Eq. 8) and the threshold friction velocity. Budd (1966) and Schmidt (1982) report that the distribution of ice particle diameters follows a two-parameter gamma function that varies with height from the ground, with α value varying between 2 and 14. However, for simplified implementation, following Déry and Yau (2002), we used a
340 constant $\alpha = 4$, which does not vary with height; this influences the modelled snow mass flux at different heights. Furthermore, the use of constant snow grain properties in the calculation of snow mobility index used in the calculation of the threshold friction velocity (Eq. (4)) can influence the spread in the data. Irrespective of these simplifications, RpNew reasonably accurately predicts the blowing snow fluxes.

Improving the blowing snow prediction is expected to improve the near-surface humidity predictions. Figure 4(a), (b), and
345 (c) present a comparison of observed relative humidity with respect to ice against the simulated relative humidity for the three experiments. Figure 4(a) shows that the NO-DRIFT case shows a negative bias in the moisture, with low $R^2 = 0.07$ (p-value < 0.01) and a high error indicated by an RMSE of 18.84%. With Rp3, the results are slightly improved with a lower negative bias and a higher $R^2 = 0.35$ (p-value < 0.01). However, Figure 4(c) shows that with RpNew, the modelled results show an improved correlation with the observations ($R^2 = 0.49$, p-value < 0.01). Though the data has a large spread, the RMSE is
350 6.6%, and the figure shows an improved match between the observed and simulated data. It is evident from Figure 4(a), (b),

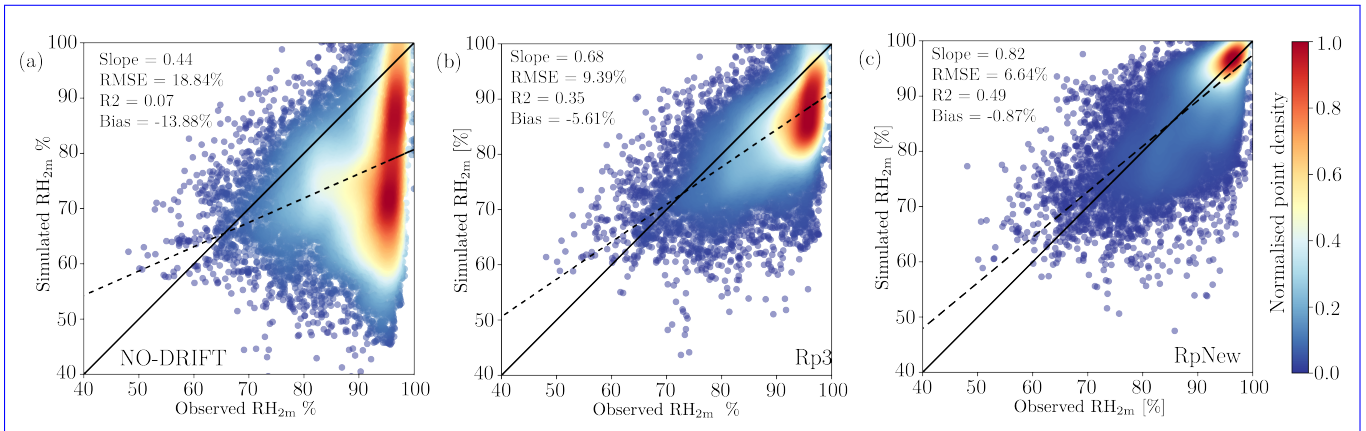


Figure 4. Density scatter plots of observed and simulated near-surface relative humidity w.r.t ice at site D47, for cases (a) NO-DRIFT, (b) Rp3, (c) RpNew. Solid lines represent the 1:1 line and the dashed lines represent the best-fit line. The colours represent the normalised point density from low (0.0, black) to high (1.0, red).

and (c) that the updates improve the moisture prediction when compared with the observations.

4.1.2 Blowing snow mass flux at site D47

In Figure 4(d) and (e), we present the comparison of simulated near-surface blowing snow mass flux with observed flux for Rp3 and RpNew, respectively. Simulated flux from Rp3 has a positive bias, with a very low R^2 indicating that Rp3 fails to capture the variability in the blowing snow flux observations. The predictions with Rp3 also have a higher RMSE of $0.035 \text{ kg m}^{-2} \text{ s}^{-1}$. Also, it is apparent from Figure 4(d) that Rp3 fails to predict the blowing snow fluxes reliably when compared with the observations. In contrast, with RpNew, we have a reasonable agreement between the observed and simulated fluxes (Fig. 4(e)) with $R^2 = 0.56$. The agreement indicates that the changes introduced in RACMO significantly improve its ability to predict the blowing snow fluxes reliably. Though the predictions are considerably improved compared to the observations, RACMO underpredicts the blowing snow fluxes. The underprediction is partially due to the under-prediction of velocities reported in table A1 and the model sensitivity to the chosen parameters. Since the snow transport flux varies in a power-law fashion with the wind speed (Radok, 1977; Budd, 1966; Amory, 2020), the flux is highly sensitive to the wind-speed predictions; even a slight underprediction in the velocity introduces a significant difference in the blowing snow mass flux. Figure 3(a) presents the instantaneous blowing snow mass flux obtained from Rp3 compared with the observations for the year 2011. It is evident from the figure that Rp3 does not reliably predict the blowing snow magnitude. In RACMO2.3p2 and Rp3, the linear saltation coefficient c_{salt} (Eq. (2)) was reduced (van Wessem et al., 2018) which resulted in the low, capped snow transport flux seen in Figure 3(a). As halving c_{salt} roughly led to halving the snow drift flux, the RACMO versions preceding version 2.3p2, with doubled c_{salt} , overestimated Q_T for most of the time (not shown). Figure 3(b) presents the instantaneous blowing snow mass flux obtained with the RpNew for the year 2011. It is evident from the figure that the RpNew works reasonably well in

predicting both the magnitude and occurrence of the blowing snow. Specifically, the flux matches the observations reasonably well in the Antarctic winter (March–October). However, it is under-predicted in the Antarctic summer (October–March). Underprediction might be related to the amount of loose snow available at the surface, possibly due to inaccuracies of the modelled surface snow compaction in summer or the direct interaction between precipitation and snow drift, which RACMO does not resolve. As we found no clear cause for the underestimation of snow drift during summer, further study is necessary to uncover the seasonal differences in the blowing snow flux. From Figures 3(a) and (b), it is evident that RpNew successfully predicts the blowing snow mass flux reliably, in contrast to Rp3, and can be used to obtain reliable continent-wide estimates of sublimation in the polar regions. Figure 3(c) presents the variation of blowing snow mass flux with the near-surface wind speed. As mentioned previously, blowing snow mass flux is expected to vary in a power-law fashion with the wind speed. Clearly, flux from Rp3 fails to produce this behaviour; however, RpNew successfully predicts the power-law variation of the blowing snow mass flux. The primary reason for this improvement is the non-uniform ice particle radius distribution, allowing us to include all relevant ice particles in the range between 2 to 300 μm . Coupled with the better coupling with RACMO prognostic variables and sub-stepping, the behaviour of the flux follows the expected power-law variation seen in Figure 3(c). Though RpNew results show the desired behaviour, it fails to capture the spread in the observational data. Through sensitivity analysis of the data, we found that the spread in the data depends on the modelling choices made, e.g. the parameter α in two-parameter gamma distribution (equation 8) and the threshold friction velocity. Budd (1966) and Schmidt (1982) report that the distribution of ice particle diameters follows a two-parameter gamma function that varies with height from the ground, with α value varying between 2 and 14. However, for simplified implementation, following Déry and Yau (2002), we used a constant $\alpha = 4$, which does not vary with height; this influences the modelled snow mass flux at different heights. Furthermore, we use constant snow grain properties with dendricity $d = 0.5$ and sphericity $s = 0.5$ in the calculation of snow mobility index MO (Lenaerts et al., 2012); these snow grain properties influence the calculation of the threshold friction velocity (Eq. (4)) which can cause different snow flux at same velocities, influencing the spread in the data. These simplifications inherent in the blowing snow model affect the model results; regardless of simplifications, it is evident from the results that RpNew successfully predicts blowing snow fluxes with reasonable accuracy.

4.1.2 Blowing snow events at site D47

To quantify the ability of RACMO to predict a blowing snow event accurately to model the blowing snow events, we follow Amory et al. (2017, 2021) and classify blowing snow events as the occurrences when the blowing snow mass flux is greater than $10^{-3} \text{ kg m}^{-2} \text{ s}^{-1}$. Subsequently, we create confusion matrices comparing the blowing snow events from observed and simulated data. The diagonal entries in the confusion matrix represent the blowing snow events correctly predicted by the simulations, and the off-diagonal entries represent the events not correctly predicted by the simulations remaining events.

Table 1(a) and (b) represent the confusion matrices that provide represents the confusion matrix presenting the percentage of blowing snow events observed and simulated by the RpNew and Rp3, respectively. In table Table 1(a), we see that out of the total observations, there are 80% of observed blowing snow events, and RpNew manages to predict 54% of these blowing snow events. In contrast, Rp3 manages to predict predicts 63% of the total blowing snow events. We calculate the blowing

405 snow frequency as the ratio of correctly simulated blowing snow events and the total number of observed blowing snow events. For RpNew, we obtain a blowing snow frequency of 0.68, and Rp3 has a blowing snow frequency of 0.79. Rp3 performs comparatively better in predicting the blowing snow events as the threshold friction velocity calculated in Rp3 is lower than RpNew. As mentioned previously, in Rp3, u_* was recalculated in every step with a simple logarithmic-law assumption, which reduced the threshold friction velocity used in the model to trigger a blowing snow event. Since the assumption was not
410 correct, we changed it and used the friction velocity calculated from the physics module. With RpNew, the model's friction velocity is consistently higher than Rp3 (not shown here). This can be tuned in future versions to match the observations better. Furthermore, we do not observe any seasonality in the underestimation of blowing snow events, we observe only marginal differences in the blowing snow frequency of RpNew over Antarctica summer (October–March) and winter (April–September) months. Clearly, Rp3 ~~manages to identify most of~~ does a better job in identifying the blowing snow events, however Fig. 3(a)
415 shows that it does not capture any peaks in the blowing snow fluxes.

To evaluate the performance of RpNew in identifying the higher magnitude blowing snow fluxes, we create another confusion matrix where we compare the blowing snow events with blowing snow mass flux $Q_T > 0.05 \text{ kg m}^{-2} \text{ s}^{-1}$. ~~Table ??(a) and (b) present~~ $\text{kg m}^{-2} \text{ s}^{-1}$. Table 1(b) presents a comparison of the observed and simulated blowing snow fluxes for events with $Q_T > 0.05 \text{ kg m}^{-2} \text{ s}^{-1}$. The tables show that 14% of the observed events account for events with high blowing
420 snow mass flux. While RpNew captures 5% out of the 14% high blowing snow events, Rp3 does not capture any of these events. ~~Specifically, RpNew successfully predicts 36% of the observed events with a high blowing snow mass flux, a marked improvement~~ Therefore, RpNew shows a marked improvement in predicting blowing snow peaks compared to Rp3. ~~This underprediction of strong snow drift events~~ However, RpNew still underestimates the number of strong blowing snow events which is closely related to the underestimation of the wind speed (Table A1) ~~as there is no apparent underestimation in the~~
425 ~~modelled strength of snow drift events when plotted as a function of the near-surface wind speed (Fig. 3e) in RpNew and Rp3.~~ The results show that RpNew provides reasonable estimates of low- and high-magnitude blowing snow events while future improvements are needed.

4.1.3 Blowing snow sublimation at site D47

Figure 5(a) shows the modelled instantaneous profiles of blowing snow sublimation rate for 2011 at site D47. In the ~~winter~~ Antarctic
430 winter (April–September), deep blowing snow layers are modelled, with a typical range of blowing snow layer heights and snow sublimation between 100 and 500 m. ~~In summer, a~~ A shallower blowing snow layer is ~~modelled. The Figure observed in~~ Antarctic summer (October–March). The figure shows multiple events with continuous blowing snow storms in winter, indicating a significant contribution of blowing snow to Antarctic sublimation. Although sublimation over a thick layer coincides with blowing snow events (Fig. 3b), we do not see a direct relation between the near-surface snow drift flux and the intensity
435 or total magnitude of blowing snow sublimation. This shows the necessity to explicitly couple the blowing snow model to the atmospheric model layers, as the modelled temperatures, humidities, and wind speeds of the lowermost model level are unlikely representative of the whole boundary layer.

Figure 5(b) presents the yearly averaged blowing snow sublimation rate profile for ~~the year~~ 2011 at site D47. The average

Table 1. Confusion matrix presenting the comparison between observed and simulated blowing snow events. [Table \(a\) considers all snow drift events.](#) [Table \(b\) on strong snow drift events.](#) In (a), DRIFT represents the events where $Q_T > 10^{-3}$ [$\text{kg m}^{-2} \text{s}^{-1}$ $\text{kg m}^{-2} \text{s}^{-1}$] and NO-DRIFT represents the remaining events.

(a) RpNew

SIM \ OBS	NO-DRIFT	DRIFT
NO-DRIFT	18% 2% DRIFT 26% 54% Rp3 NO-DRIFT DRIFT NO-DRIFT 16%	2% 4%
DRIFT	26% 17%	54% 63%

Confusion matrix presenting the high mass flux blowing snow events.

Diagonal elements represent the events that are correctly classified between observations and simulations.

(b) RpNew

SIM \ OBS	$Q_T \leq 0.05$	$Q_T > 0.05$
$Q_T \leq 0.05$	84% 86%	2% 0%
$Q_T > 0.05$	9% 14%	5% 86% Rp3 $Q_T \leq 0.05$ $Q_T > 0.05$ $Q_T \leq 0.05$ 0%
$Q_T > 0.05$	14% 0%	

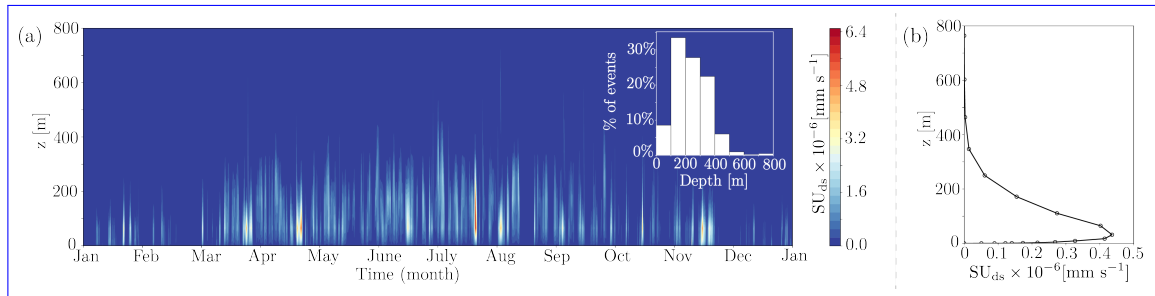


Figure 5. (a) [Blowing snow sublimation rate for the year 2011 in \$\text{mm s}^{-1}\$](#) , inset shows the [histogram of blowing snow layer depth \(m\)](#). (b) [Yearly averaged of blowing snow sublimation rate with height \(\$\text{mm s}^{-1}\$ \)](#).

blowing snow layer depth is 230 ± 116 mm. As the air is saturated at the surface, the sublimation at the surface is negligible, with sublimation increasing away from the ground and maximum sublimation above. Déry and Yau (2002) and Toumelin et al. (2021) have reported a similar variation of the blowing snow sublimation. It is worth noting here that both the drifting snow concentration and horizontally drifting snow transport are peaking even close to the ground (not shown). As depicted in Figure 5(a), blowing snow sublimation starts well below the first RACMO model level as the lowermost PIEKTUK model layers are saturated with respect to water vapour. Blowing snow sublimation thus occurs in the upper part of below the boundary layer, where the blowing snow concentration is low, but the air is not yet saturated model's first atmospheric level (approximately 8–10 m). Previously in Rp3, this vertical profile of sublimation was not represented as the blowing snow sublimation was added to the surface.

Based on lidar data from CALIPSO (~~Cloud-Aerosol-Lidar-and-Infrared-Pathfinder-Satellite-Observation~~)observations, Palm et al. (2017) report for the Antarctic Ice Sheet north of 82 °S an average snow layer depth of 120 m, with typical blowing snow layers of 200 m all along the coastal katabatic wind regions (see Fig. 5 in Palm et al. (2018)). For the site D47, RpNew shows a similar mean layer depth of 230 ± 116 mm, and a similar typical range (Inset Fig. 5(a)). This analysis shows that RpNew satisfactorily reproduces all the necessary features of the blowing snow sublimation and can be used to obtain continent-wide estimates. However, it is worth mentioning that total blowing snow sublimation is sensitive to horizontal resolution. At the 27 km resolution employed in the study, strong spatial gradients near the coast would not be accurately captured. Subsequently, the impact of blowing snow on sublimation and horizontal transport of mass can be underestimated.

~~Yearly mean (2011): (a) Yearly average blowing snow sublimation rate for the year 2011 in mm s^{-1} , inset shows the histogram of blowing snow layer depth (m). (b) Variation of blowing snow sublimation rate with height (mm s^{-1}).~~

4.2 Continental blowing snow frequency

Figure 6 gives the monthly variation of mean blowing snow frequency over Antarctica for the decade 2001–2010. Blowing snow frequency is obtained by calculating all the blowing snow events with the blowing snow mixing ratio $q_b > 10^{-6} \text{ kg kg}^{-1}$ $q_b > 10^{-6} \text{ kg kg}^{-1}$. The cutoff q_b , the limits, and the colourmap in Figure 6 are chosen to facilitate a qualitative comparison with the satellite observations presented in Figure 3 in Palm et al. (2018). We observe that the monthly blowing snow frequency largely follows the seasonal trend in the surface wind patterns over Antarctica, with high-frequency blowing snow in winter compared to summer. ~~Whereas Figure 3(b) suggests that RpNew underestimate summer snow drift, such summer underestimation is not very apparent between RACMO and the satellite observations. It is worth mentioning here that the blowing snow frequency presented in Figure 6 includes near-surface blowing snow flux. In contrast, the satellite observations by Palm et al. (2018) include only those blowing snow layers deeper than 30 m and only those events without clouds.~~ Despite the differences between the two approaches, the simulated blowing snow frequency is qualitatively similar to that obtained from the CALIPSO satellite observations (Palm et al., 2017, 2018). The results show a persistent blowing snow hotspot in East Antarctica near Adélie Land, observed in satellite observations and our simulations. We can also infer that the satellite observations slightly underpredict underestimate the frequencies compared with the simulations ~~for the reasons above~~ due to the reasons mentioned in Section 3.2.

Our results are also qualitatively similar to the simulations with the CRYOWRF model carried out by Gerber et al. (2023): ~~Though there are differences between the studies, the results are qualitatively comparable, although the simulated periods are different.~~ Most of the blowing snow hotspots observed in our simulations also correspond to the ‘wind glaze’ areas in East Antarctica reported by Scambos et al. (2012). Scarchilli et al. (2010) report blowing snow frequencies of 80% at the wind convergence zone of Terra Nova Bay (East Antarctica); we observe approximately 80–90% blowing snow frequency in the area during the Antarctic winter months.

~~Yearly averaged (2000-2010) difference between RpNew and Rp3 quantities: (a) Blowing snow sublimation mm yr^{-1} , (b) Blowing snow transport $\text{kg m}^{-1}\text{yr}^{-1}$, (c) Near-surface temperature T_{2m} in $^{\circ}\text{C}$, (d) Relative humidity in percentage, (e) Total~~

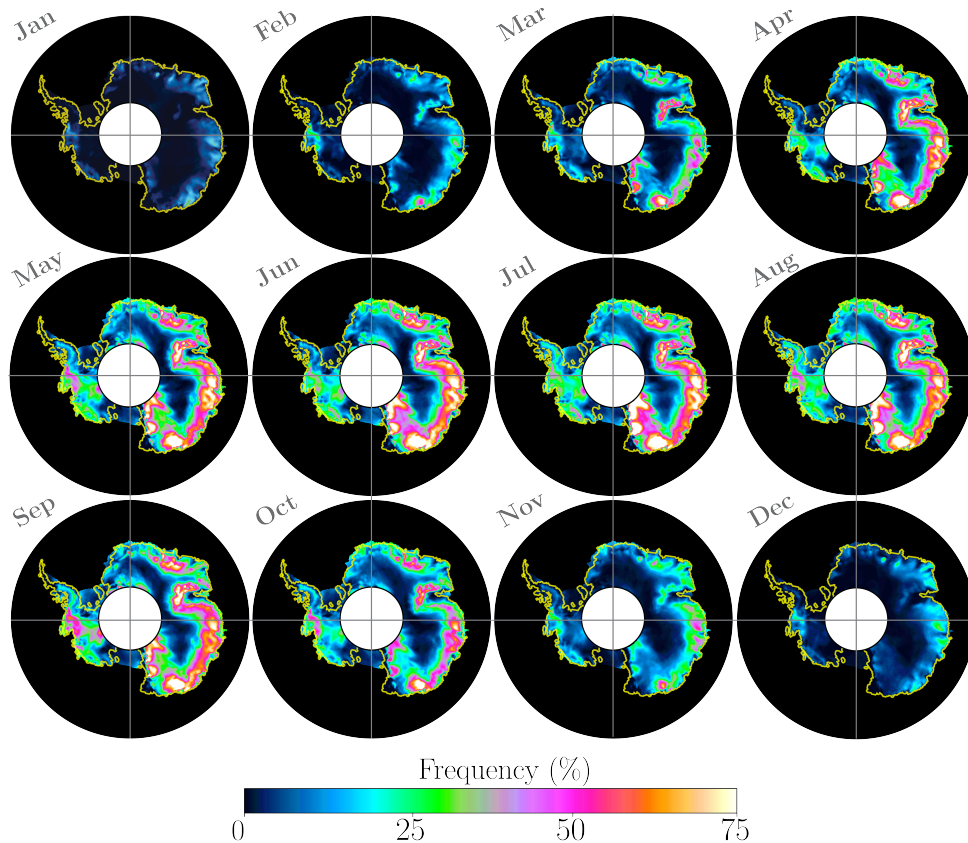


Figure 6. Blowing snow frequency visualised to provide a qualitative comparison with satellite measurements of Palm et al. (2018). [Figures The panels](#) show average blowing snow frequency over the decade 2001–2010 [and use the same colour scale as Palm et al. \(2018\). A colour blind friendly version of this figure is given in the appendix \(Figure B1\).](#)

sublimation mm yr^{-1} , and (f) SMB mm yr^{-1} . SU_{ds} , SU_{total} , and SMB are in mm water-equivalent. (g) Instantaneous drifting snow flux at an interior region of East Antarctica (71.1°S , 111.7°E).

4.3 Difference between RpNew and Rp3

In Figure C1, we present the difference in some important variables between RpNew and Rp3 to quantify the magnitude of change between the two versions. The blowing snow transport TR_{ds} (Fig. C1(b)) decreased somewhat over most of Antarctica with significant but localised increases in transport along George V Land, Adélie Land, and Dronning Maud Land. At these locations, the blowing snow transport is increased by 2–3 times compared to Rp3 due to better modelling of snow particle distribution, which includes more particles with well-distributed ice particle radii and particle initialisation. As visualised in Figure C1(g) as an example, however, for most of Antarctica, most blowing snow events are reduced in intensity by the model updates. Only a few instances per year does the wind speed exceed the threshold for which the updated blowing snow model

simulates higher blowing snow transport. Conversely, for most of Antarctica, we observe higher blowing snow sublimation (Fig. C1(a)) due to the ability of RpNew to capture the peaks in blowing snow fluxes and the change in initialisation employed for the blowing snow model. This increase indicates the necessity of a direct two-way coupling of the modelled atmospheric profile of the surface layer to the blowing snow model. In the RpNew, the snow particles are lifted into the warmer and drier air of the upper part of the stable boundary layer. In Rp3, particles were not lifted that high – due to errors in the particle size distribution – not seeing this warmer air due to using an extrapolated 10 m temperature profile assuming neutral conditions. The larger ice shelves are the only regions of Antarctica where blowing snow sublimation decreases. Here, the stable boundary layer is generally very thick (e.g. van den Broeke and Van Lipzig (2003), Fig. 10), inhibiting the blowing snow from reaching the warmer air above the surface layer. Results show RpNew is slightly colder by 0.3–0.4 K (Fig. C1(e)) along the coastal areas when compared to Rp3. This results from a better coupling of blowing snow sublimation to the tendencies of temperature, which allows the removal of latent heat from upper vertical levels of RACMO. Compared to Rp3, RpNew has higher relative humidity (Fig. C1(d)) also, due to better coupling of blowing snow moisture tendencies with RACMO, the change in moisture leads to an increase in the dew-point temperature of 2–4 K (not shown here) in the first few vertical layers of RACMO. Furthermore, the total sublimation is higher in RpNew (Fig. C1(e)) when compared to Rp3. Along the coast, the difference is as high as 100 mm w.e. yr⁻¹. Overall, the averaged surface mass balance (Fig. C1(f)) is changed mostly along the coastal Antarctica with a reduction of approximately 30–40 mm w.e. yr⁻¹. Since there is an increase in the moisture availability, there is relatively higher precipitation over Ronne and Ross ice shelves with a corresponding increase in SMB of approximately 20 mm w.e. yr⁻¹. In conclusion, changes introduced in RpNew greatly influence the overall sublimation pattern in Antarctica and moisture content in lower levels of the atmosphere. In the RpNew, blowing snow’s impact is more regional than Rp3. However, the overall impact on SMB is limited, with a decrease in SMB on the Eastern Antarctic coast and a slight increase in SMB in Western Antarctica due to higher moisture content created by blowing snow sublimation.

4.3 Continent-wide estimates of blowing snow climate over Antarctica

Yearly mean (2000-2010): (a) Blowing snow sublimation SU_{ds} in mm water equivalent, (b) Difference in near-surface temperature, ΔT_{2m} between RpNew and NO-DRIFT simulations, (c) Difference in relative humidity ΔRH_{2m} , (d) Blowing snow flux $kgm^{-1}yr^{-1}$, (e) Erosion due to blowing snow, ER_{ds} or the divergence due to blowing snow $kgm^{-1}yr^{-1}$, and (f) Total sublimation SU_{total} , including surface and blowing snow sublimation $kgm^{-1}yr^{-1}$. Figure 7 presents the updated continent-wide estimates of the blowing snow climate of Antarctica by comparing the yearly average (2000-2010 2000-2012) quantities of RpNew and NO-DRIFT simulations. Similar to previous model results (Lenaerts and van den Broeke (2012)), we observe negligible blowing snow sublimation (Figure 7(a)) in the interior parts of Antarctica with maximum sublimation towards the coast. Model results show blowing snow sublimation hotspots ($SU_{ds} > 100 \text{ mm w.e. yr}^{-1}$ $SU_{ds} > 100 \text{ mm w.e. yr}^{-1}$) in George V Land, Adélie Land, Wilkes Land, and Queen Mary Land in Eastern Antarctica with non-zero sublimation all along the coast of Antarctica. RACMO shows negligible sublimation over Dome Fuji, Dome Argus, and Dome C, which form the interior parts of Eastern Antarctica, due to the lower wind speed and low temperatures in these regions (Fig. 1(a)). Similarly, we observe negligible sublimation over Ronne and Ross ice shelves, which also experience low wind speeds. This shows that blowing

525 snow sublimation is mostly limited to the katabatic wind regions of Antarctica. Maximum blowing snow sublimation of $335 \pm 30 \text{ mm w.e. yr}^{-1}$ occurs in Adélie Land at the location 66.9°S , 130.4°E . Palm et al. (2017) based on the CALIPSO lidar observations report a maximum blowing snow sublimation of $250 \pm 125 \text{ mm w.e. yr}^{-1}$ near the coast between longitudes 140 and 150°E . A slight shift in the location of the maximum blowing snow sublimation between the satellite and model results can be related to the fact that CALIPSO observes moderate and strong events without thick cloud
530 cover, while Figure 7 displays all snowdrift events (see Section 3.2). Both spatial distribution and the magnitude of blowing snow sublimation from RpNew match reasonably well with CALIPSO observations of Palm et al. (2017).

Figure 7(b) provides the difference between the 2-meter temperature for the RpNew and NO-DRIFT cases. The figure shows that blowing snow sublimation reduces the near-surface temperature. At blowing snow sublimation hotspots, we observe a cooling of $0.1 - 0.3 \text{ K}$, with negligible change in the temperature over most of interior Antarctica. It is worth mentioning here that
535 with Rp3, we observed a ~~‘warm’~~ slight warm bias compared to the case with NO-DRIFT (not shown); this shows that the coupling was ~~incorrect in the previous version of RACMO~~ previously incorrect. The results have appreciably improved with RpNew. However, the overall effect of blowing snow sublimation on the yearly average near-surface temperature in Antarctica seems negligible-marginal, similar to previous model results.

Higher sublimation due to blowing snow in RpNew ~~to lead to~~ leads to higher near-surface relative humidity (Fig. 7(c))
540 when compared to NO-DRIFT simulations. We observe higher relative humidity along the Antarctic coast with a maximum of 10% in the coastal George V Land and Adélie Land. This increase in relative humidity is higher ~~when compared to~~ than what was previously observed with RACMO Rp3. Similar to sublimation, blowing snow transport TR_{ds} ($\text{kg m}^{-1} \text{ yr}^{-1}$) (Fig. 7(d)) is negligible over interior Antarctica. We observe a strong blowing snow transport near coastal George V Land with maximum transport of $9 \times 10^6 \text{ kg m}^{-1} \text{ yr}^{-1}$. Along the rest of the Antarctic coast, blowing snow transport is approximately $2 \times 10^6 - 3 \times 10^6 \text{ kg m}^{-1} \text{ yr}^{-1}$. Blowing snow erosion ER_{ds} (mm w.e. yr^{-1}) (Fig. 7(e))
545 which is a contributor to Antarctic SMB, shows complex convergence and divergence patterns all along the Antarctic coast. Similar to Bromwich et al. (2004) and Lenaerts and van den Broeke (2012), we observe large blowing snow divergence near escarpment areas with significant katabatic wind acceleration. Furthermore, areas with blowing snow convergence are near blowing snow divergence, which indicates that blowing snow is important for redistributing the precipitation in the coastal
550 areas of Antarctica. However, the magnitude of ER_{ds} is not significant enough for a major contribution to SMB, as only the snow blown off Antarctica counts for the integrated SMB.

Total sublimation SU_{total} (mm w.e. yr^{-1}), the sum of blowing snow and surface sublimation ($\text{SU}_{\text{ds}} + \text{SU}_{\text{s}}$), follows the spatial distribution of blowing snow sublimation. Maximum total sublimation of $396 \text{ mm w.e. yr}^{-1}$ is observed at the same location as the maximum blowing snow sublimation, indicating the leading contribution of blowing
555 snow sublimation to the total sublimation. Total sublimation is higher in the RpNew simulations when compared to NO-DRIFT simulations (Figure 7(f)); in the regions near Adélie Land, the difference in total sublimation is as high as $200 \text{ mm w.e. yr}^{-1}$.
~~In the absence of blowing snow sublimation, total sublimation is under-predicted, and therefore, blowing snow sublimation should be included in the calculations of SMB.~~

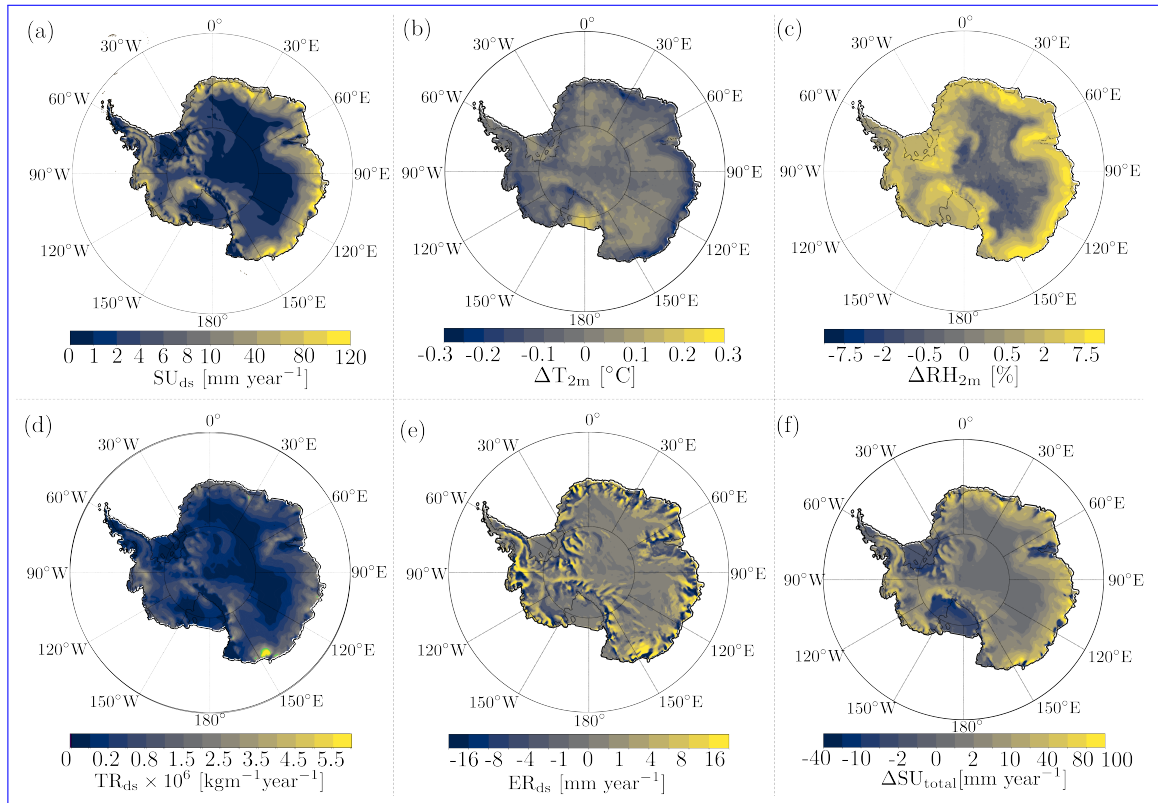


Figure 7. Yearly mean (2000–2012): (a) Blowing snow sublimation SU_{ds} in mm water equivalent, (b) Difference in near-surface temperature, ΔT_{2m} between RpNew and NO-DRIFT simulations, (c) Difference in relative humidity ΔRH_{2m} , (d) Blowing snow flux $[kgm^{-1}yr^{-1}]$, (e) Erosion due to blowing snow, ER_{ds} or the divergence due to blowing snow $[kgm^{-1}yr^{-1}]$, and (f) Total sublimation SU_{total} , including surface- and blowing-snow sublimation $[kgm^{-1}yr^{-1}]$.

4.4 Seasonal variation of integrated sublimation

560 4.5 Seasonal variation of integrated sublimation

In Figure 8 we present the different components of sublimation from RpNew, NO-DRIFT, Rp3, and CRYOWRF (Gerber et al., 2023)

Monthly contribution to the yearly average integrated blowing snow sublimation from Rp3 and RpNew (Fig. 8(a)) shows that the blowing snow sublimation is lower in summer compared to winter. Lower sublimation is in the Antarctic summer (October–March) is lower than in Antarctic winter (April–September) due to higher temperatures and summer snow densities,

565 making it difficult for the snow to lift off from the ground. Blowing snow sublimation SU_{ds} increases with the onset of winter and remains relatively constant over winter with an approximate contribution of $15 - 20 Gtmo^{-1} Gtmo^{-1}$ in winter. Constant blowing snow indicates that blowing snow sublimation is a major contributor to total sublimation in winter. Due to the updates made in RpNew, the blowing snow sublimation has nearly doubled throughout the winter compared to Rp3. CRYOWRF pro-

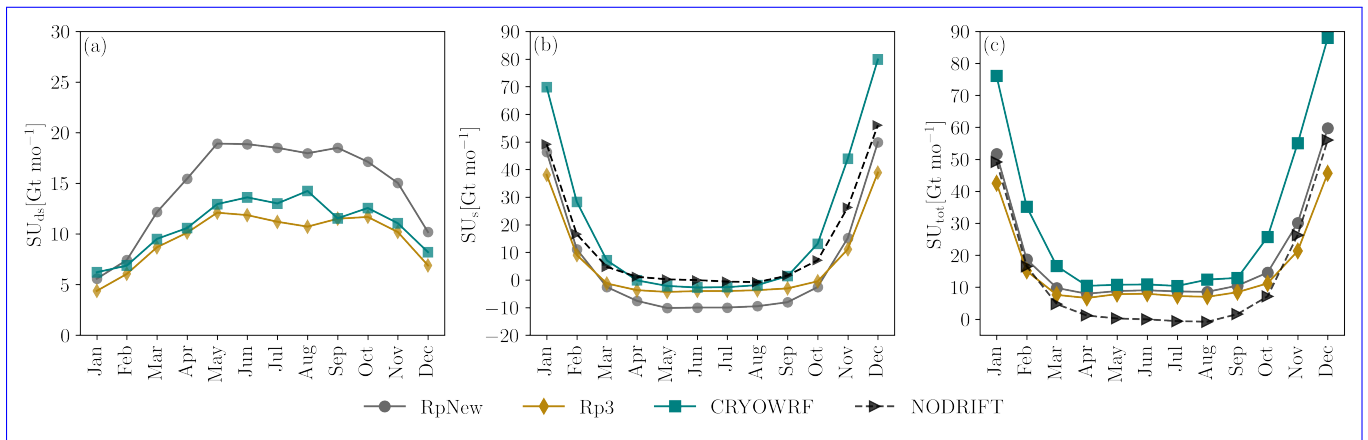


Figure 8. Monthly contribution to the yearly mean (2000–2010/2012) (all in Gt mo^{-1}) (a) integrated blowing snow sublimation over total ice sheet, (b) integrated surface sublimation, and (c) integrated total sublimation ($\text{SU}_{\text{tot}} = \text{SU}_{\text{ds}} + \text{SU}_{\text{s}}$); (d) the difference between integrated SU_{total} in the RpNew and NO-DRIFT.

duces blowing sublimation which is comparable in magnitudes to Rp3. Surface sublimation SU_{s} dominates the sublimation in summer due to higher temperatures (Fig. 8(b)) and reaches a relatively constant value in winter. We observe that surface sublimation in Antarctic summer with CRYOWRF is nearly 1.5 times the surface sublimation observed with RpNew, while winter sublimation is comparable. Surface sublimation SU_{s} dominates the sublimation in summer due to higher temperatures (Fig. 8(b)) and reaches a relatively constant value in winter. In winter, between March and November, we observe is negligible in Antarctic winter and it is nearly zero. Interestingly, with the introduction of blowing snow sublimation in Rp3 and RpNew, we observed negative surface sublimation, hence indicating the deposition of water vapour onto the snow surface in winter. This deposition agrees with the measurements of King et al. (1996), who measured small, downward water vapour fluxes in the winter of 1991 at Halley station, East Antarctica. A similar seasonal cycle in the surface sublimation with a negative surface sublimation in winter has been reported by King et al. (2001). While the blowing snow sublimation is increased in RpNew, the negative surface sublimation also increases, balancing the net change in total sublimation. The deposition follows the same spatial and seasonal pattern as the blowing snow sublimation. Since the condensation is directly proportional to the difference between the vapour pressure of water at the surface and above the surface, with RpNew, which has better coupling with the atmosphere, there is more condensation in winter compared to Rp3. Specifically, condensation in winter is nearly doubled with RpNew compared to Rp3. However, we do not see such a negative surface sublimation with CRYOWRF.

Total sublimation SU_{total} (Fig. 8(c)) follows a similar pattern as the surface sublimation, with higher values during Antarctic summer and relatively constant values in winter. Figure 8(d) presents the difference between total sublimation and surface sublimation, which shows the difference is more or less equal to blowing snow sublimation. The difference in the total sublimation between Rp3 and RpNew shows that the major sublimation changes are observed in It is clear from the NO-DRIFT case that the surface sublimation is negligible in Antarctic winter. The magnitude of total sublimation is comparable between RpNew and CRYOWRF in the Antarctic winter (March–September); the difference in the sublimation between different models

590 is mostly a summer phenomenon. CRYOWRF consistently produces higher summer ~~, with higher sublimation in summer with~~
~~sublimation values than~~ RpNew. While the seasonal trends of the sublimation remain unaltered between Rp3 and RpNew,
 interestingly, we observe that an increase in blowing snow sublimation in ~~RpNew in~~ winter leads to an increase in deposition,
 leading to ~~marginal limited~~ overall changes to total sublimation. ~~However, as Figure C1(e) shows, these limited changes in the~~
~~spatially mean sublimation result from rather large but opposing regional changes in total sublimation.~~

595 4.5 Changes in integrated SMB

Table 2. Total ice sheet, including ice shelves, integrated SMB mean 2000–~~2010~~2012 values (Gt yr^{-1} – Gt yr^{-1}) with interannual variability σ :
 total (snow and rain) precipitation (P_{tot}), total sublimation (SU_{tot}), surface sublimation (SU_{s}), blowing snow sublimation (SU_{ds}), blowing snow
 erosion (ER_{ds}), run-off (RU). ~~ER_{ds} only considers the transport aspect of blowing snow. ER_{ds} is positive in case of erosion due to divergence of~~
~~the blowing snow flux, and negative if convergence of the blowing snow flux brings snow to a grid box. Furthermore, as ER_{ds} only considers~~
~~the snow redistribution, the spatially integrated impact on the SMB is zero as long as drifting snow is not blown off the ice sheet.~~ Integrated
 surface mass balance is given by: $\text{SMB} = P_{\text{tot}} - SU_{\text{ds}} - SU_{\text{s}} - ER_{\text{ds}} - \text{RU}$. (a) ~~Difference Change~~ between RpNew and ~~RP3NO-DRIFT~~,
~~Percentage change is calculated as (RpNew - NO-DRIFT)/NO-DRIFT~~, and (b) SMB difference between RpNew (~~2000-2010~~2000-2012)
 with CRYOWRF (2010–2020) (Gerber et al., 2023)

	(a) RpNew (2000–2010 2000–2012) and RP3NO-DRIFT (2000–2012)				(b) RpNew (2000–2010 2000–2012) and CRYOWRF (2010–2020)					
	NO-DRIFT		RpNew		RpNew - NO-DRIFT		RpNew		CRYOWRF	
	mean	σ	mean	σ	mean (% change)	mean	σ	mean	σ	mean
P_{tot}	2696 2622	97 96	2674 2678	99 96	+22(0.8%) 56(2.1%)	2696 2678	97 96	3101	-	-405(-14%) -423
SU_{tot}	237 161	10 8	188 234	5 10	+49(23%) 76(47%)	237 234	10	335	-	-98(-34%) -101
SU_{s}	61 161	8	72 59	5 8	-11(-16%) 102(-63%)	61 59	8	234	-	-173(-117%) -175
SU_{ds}	176	7	116 175	4 7	+60(34%) 176(100%)	176 175	7	101	-	+75(54%) +74
ER_{ds}	-	-	8	0.5	5.0(2.1%) 8(3%)	-	8	0.5	-	-23(-118%) -23
RU	7	3	7	3	RU	7	3	5	-	+2(+33%)
SMB	2444 2454	100 95	2474 2428	99 96	-30(-1.2%) SMB(-124%)	2444 2428	100 96	2730	-	-286(-11%) -302

Table 2(a) presents the SMB and its components integrated over the whole ice sheet (including ice shelves) for the years
 2000 – ~~2010 in~~ Gt yr^{-1} –~~2012 in~~ Gt yr^{-1} along with their inter-annual variability. Compared to ~~RP3NO-DRIFT~~, RpNew has
 an increased precipitation of ~~22~~ Gt yr^{-1} –~~56~~ Gt yr^{-1} caused by the higher moisture content in the atmosphere due to ~~higher~~
 blowing snow sublimation. The total sublimation is increased by ~~49~~ Gt yr^{-1} –~~76~~ Gt yr^{-1} with blowing snow sublimation being
 the major contributor. There is a ~~slight~~ decrease in surface sublimation (~~11~~ Gt yr^{-1}) as ~~air in the boundary layer is saturated~~
~~more efficiently with RpNew compared to Rp3, which causes a reduction in the potential for the surface of~~ ~~102~~ Gt yr^{-1} as
 blowing snow sublimation is now the dominant mechanism of sublimation. With ~~higher~~ blowing snow transport fluxes, we
 have a ~~higher~~ snow erosion increase of ~~3~~ Gt yr^{-1} . ~~This number remained small as snow erosion only influences the integrated~~
~~SMB once the snow is blown off the ice sheet.~~ ~~8~~ Gt yr^{-1} . Overall, the integrated SMB is reduced by ~~30~~ Gt yr^{-1} –~~26~~ Gt yr^{-1} ,

605 due to a net increase in blowing snow sublimation. The change amounts to only a ~~1.21~~1.21% decrease in SMB compared to ~~Rp3~~the
NO-DRIFT case. Since the change in SMB with the updates is minor and the SMB results from RACMO have been previously
evaluated against several in-situ and remote sensing observations, we refer to Noël et al. (2018); van Wessem et al. (2018) for
the SMB evaluation. Though there is negligible change in the overall SMB, blowing snow sublimation is highly important to
local SMB, especially in the escarpment areas in Eastern Antarctica.

610 ~~Recently Gerber et al. (2023) carried out simulations of Antarctic climate at 27 km resolution using the CRYOWRF model.~~
Table 2(b) compares the integrated quantities obtained from RpNew with ~~CRYOWRF. It is worth noting here that the experiments~~
~~with CRYOWRF were carried out from 2010 to 2020, while our results are for 2000 to 2010. While the time~~the results from
CRYOWRF from 2010–2020. While the period is different, Gerber et al. (2023) is the only other study (other than RACMO
studies) that reports SMB results of the entire Antarctica with a blowing snow model, making these results interesting to com-
615 pare. ~~Table 2(b) shows that there is a large difference in SMB (11%) and precipitation (14%) between RpNew and CRYOWRF.~~
~~While precipitation and SMB are comparably higher in CRYOWRF, the ablation terms of CRYOWRF, especially sublimation,~~
~~are more interesting. Specifically, CRYOWRF produces higher total sublimation (+129 G_{tyr}⁻¹) when compared to RpNew.~~
~~While we observe in RpNew that the surface sublimation is reduced in the presence of blowing snow sublimation, such a~~
~~trend is not visible in CRYOWRF results. Furthermore, the difference in erosion due to snow being blown off Antarctica is~~
620 ~~significant.~~Our experience with RACMO runs suggest that the total sublimation from Rp3 does not vary much in the decade
between 2000-2020. Therefore, we do not expect a large difference in sublimation during this time period, and therefore, the
results are comparable. Table 2(b) shows that there is a large difference in SMB (11%) and precipitation (14%) between Rp-
New and CRYOWRF. While precipitation and SMB are comparably higher in CRYOWRF, the ablation terms of CRYOWRF,
especially sublimation, are more interesting. Specifically, CRYOWRF produces higher total sublimation (+101 G_{tyr}⁻¹) when
625 compared to RpNew. From monthly average sublimation (Fig. 8) we observed that the CRYOWRF produces higher surface
sublimation in Antarctic summer (October–March), when compared to winter.

5 Summary and conclusions

In this study, we updated the blowing snow model in the regional climate model RACMO, version 2.3p3 (Rp3), to better repre-
630 sent the blowing snow phenomenon, the major ablation term in the SMB of the Antarctic ice sheet. As observed in the limited
available observations, the unaltered version of the model Rp3 failed to accurately predict the power-law variation of blowing
snow mass flux with wind speed~~compared to observations~~. Furthermore, choices made in the unaltered version to reduce the
~~computational expenses of the~~ blowing snow model's computational expenses led to simplifications and assumptions ~~which~~
that affected the model results. In the present work, we updated the empirical formulation of saltation flux used as the boundary
635 condition for the blowing snow model. We increased the number and distribution of ice-particle radius classes to cover all the
relevant blowing snow ~~radii~~radius classes. We also improved the coupling of the blowing snow model with RACMO by pro-
viding velocity, temperature profiles and friction velocities from RACMO to the blowing snow model, which was previously

being modelled as a logarithmic-law velocity and the friction velocity was based on the first model level velocities. In addition, we found that the blowing snow model was very sensitive to its time step and introduced sub-stepping for the blowing snow model, which significantly improved the results.

We ran the original blowing snow model (Rp3) and the updated code (RpNew) for Antarctica on a 27 km grid laterally forced by 3-hourly ERA5 data. We performed three experiments for ~~2000–2010: Rp3~~2000–2012: NO-DRIFT, RpNew, and ~~NO-DRIFT~~Rp3. In the ~~last experiment~~experiment NO-DRIFT, RACMO was run without the blowing snow model. The results from the updated model were evaluated against in-situ ~~observation~~observations from site D47, Adélie Land, Antarctica (Amory, 2020). Important surface quantities such as the near-surface wind, temperature, humidity and blowing snow fluxes were compared. We found that RpNew results compared well against the blowing snow observations, successfully predicting both blowing snow frequency and magnitude. Furthermore, RpNew also successfully predicts the power-law variation of the blowing snow transport fluxes with wind speed. Comparison of continental blowing snow frequency obtained from RpNew with CALIPSO satellite observations (Palm et al., 2018) shows that qualitatively, RpNew predicts the blowing snow frequency over Antarctica reasonably well.

The updated estimates of blowing snow sublimation from RpNew also agree well with the continent-wide estimates of blowing snow sublimation from satellite observations. Average blowing snow depth of 230 ± 116 ~~mm~~m obtained from RpNew matches reasonably well with the satellite observations from Palm et al. (2017). Furthermore, Palm et al. (2017) from CALIPSO lidar observations report a maximum blowing snow sublimation of 250 ± 125 ~~mm w.e. yr⁻¹~~mm w.e. yr⁻¹ near the Antarctic coast around 140°E longitude. We observe a maximum blowing snow sublimation of 335 ± 30 ~~mm w.e. yr⁻¹~~mm w.e. yr⁻¹ at the location: 66.9°S, 130.4°E. CALIPSO satellite observations indicate blowing snow sublimation could be as high as 393 ± 196 ~~Gt yr⁻¹~~Gt yr⁻¹. We observe a blowing snow sublimation of 176 ± 10 ~~Gt yr⁻¹~~Gt yr⁻¹ with RpNew which shows there is a significant difference between model results and satellite observations. Palm et al. (2018) attribute the high blowing snow sublimation estimates to the errors associated with MERRA-2 reanalysis data (Gelaro et al., 2017) used for calculating sublimation, particle radius error, and extinction errors and therefore, the satellite estimates involve a large error. However, without other continental-scale estimates of blowing snow sublimation, future studies must properly document the differences between different methods.

In the absence of blowing snow sublimation, the sublimation in Antarctica is mostly a summertime phenomenon (October–March), shown by NO-DRIFT experiment with negligible surface sublimation in winter. However, with the introduction of the blowing snow model, total sublimation increases with a large contribution of blowing snow sublimation in the Antarctic winter (April–September).

We observe an interesting self-limiting nature of total sublimation from ~~RACMO~~RpNew model results. Specifically, while the RpNew leads to an increase in the blowing snow sublimation, we observed a corresponding decrease in the surface sublimation and a non-negligible increase in deposition, balancing the total sublimation in Antarctic winter. ~~Based on RpNew results, we hypothesise that sublimation in Antarctica is a self-limiting mechanism where large blowing snow sublimation saturates the~~
In RpNew, sublimation in Antarctica is a self-limiting mechanism where large blowing snow sublimation saturates the near-surface layers, limiting the potential for surface sublimation. Future intercomparison studies with other models are necessary to test the hypothesis. We also compared RpNew result with the simulation results from CRYOWRF (Gerber et al., 2023). While

blowing snow sublimation is the major contributor to the total sublimation in RpNew, surface sublimation is the dominant contributor to total sublimation in CRYOWRF. Furthermore, sublimation in CRYOWRF is nearly four times higher than RpNew surface sublimation. The difference shows that future intercomparison studies are necessary to identify the major contributor to total sublimation.

In conclusion, the updates introduced to the regional climate model RACMO in this study significantly improve the representation of blowing snow physics within the model. Blowing snow and surface sublimation are the major mass loss terms in the SMB of Antarctica, leading locally to a negative SMB, which results in the formation of black ice areas. This study presents a step forward in modelling blowing snow to produce a physically sound and reliable estimate of the SMB of Antarctica.

Data availability. Monthly-accumulated sublimation and Yearly accumulated SMB components for NO-DRIFT, Rp3, and RpNew are publicly available on Zenodo (<https://zenodo.org/doi/10.5281/zenodo.12509004>) for the years 2000-2012. Observational data was downloaded from Amory et al. (2020b). CRYOWRF results were downloaded from Gerber et al. (2022).

Author contributions. SG and WJB conceived this study, decided on the new model settings. SG performed the code development and performed the model simulations and led the writing of the manuscript.

Competing interests. The authors declare that they have no conflict of interest.

Appendix A: Near surface climate

Table A1. Root-mean-squared-error (RMSE), slope, intercept, bias, and coefficient of determination (R^2) of comparison of NO-DRIFT, Rp3, and RpNew simulations against observations at site D47. Statistics are reported for 2-m wind speed in m s^{-1} , 2-m temperature in $^{\circ}\text{C}$, 2-m relative humidity w.r.t ice in %, and the near surface blowing snow flux in $\text{kg m}^{-2} \text{s}^{-1}$.

	NO-DRIFT				Rp3				RpNew			
	U_{2m}	T_{2m}	RH_{2m}	Q_T	U_{2m}	T_{2m}	RH_{2m}	Q_T	U_{2m}	T_{2m}	RH_{2m}	Q_T
<u>Slope</u>	<u>0.76</u>	<u>1.01</u>	<u>0.44</u>	-	<u>0.78</u>	<u>1.01</u>	<u>0.67</u>	<u>0.24</u>	<u>0.75</u>	<u>1.01</u>	<u>0.82</u>	<u>0.5</u>
<u>RMSE</u>	<u>3.84</u>	<u>3.09</u>	<u>18.84</u>	-	<u>3.69</u>	<u>3.17</u>	<u>9.39</u>	<u>0.04</u>	<u>3.88</u>	<u>3.04</u>	<u>6.64</u>	<u>0.03</u>
<u>R^2</u>	<u>0.77</u>	<u>0.91</u>	<u>0.07</u>	-	<u>0.76</u>	<u>0.91</u>	<u>0.35</u>	<u>0.24</u>	<u>0.76</u>	<u>0.91</u>	<u>0.49</u>	<u>0.57</u>
<u>Bias</u>	<u>-3.34</u>	<u>1.61</u>	<u>-13.88</u>	-	<u>-3.17</u>	<u>1.75</u>	<u>-5.61</u>	<u>0.003</u>	<u>-2.72</u>	<u>1.45</u>	<u>-0.87</u>	<u>-0.01</u>

We evaluate the performance of RpNew in predicting the near-surface layers, limiting the potential for surface sublimation. RpNew results support our hypothesis. However, results from the CRYOWRF model (Gerber et al., 2023), which also models

690 ~~the blowing snow phenomenon, do not follow this trend~~ wind speed, temperature, relative humidity, and snow transport fluxes
for 2010–2012 compared to the Rp3 and NO-DRIFT experiments. Table A1 presents the statistics comparing observed near-surface
quantities against simulated results from the three experiments. We observe that the model underestimates the near-surface
wind speed in all three experiments however with the current updates, the model bias is slightly decreased from -3.34 ms^{-1}
in the NO-DRIFT case to -2.72 ms^{-1} in the case of RpNew. Model captures the variability in the data reasonably well, with
695 negligible differences between the three experiments. The coefficient of determination (R^2) is approximately 0.76, indicating
that model results resemble the synoptic evolution of the wind strength well. A RMSE of approximately 3.88 ms^{-1} indicates
that there are still significant differences between the model results and observations. As all three simulations underestimate
the wind speed, we also performed tests with dual mass flux–TKE scheme (van Meijgaard et al., 2012), which allows better
modelling of the turbulent boundary-layer processes. However, it did not improve the wind-speed predictions appreciably (not
700 shown). Therefore, ~~future intercomparison studies with other models are necessary to test the hypothesis~~ this scheme was not
used further. The under-prediction of simulated wind speed is likely due to the lower vertical resolution of the model, wherein
the first atmospheric level is approximately 8 to 10 m above the surface, and the 2-m wind speed is calculated based on the
similarity theory and is not simulated.

~~Compared to Rp3, with an increase in~~ In the blowing snow model, the mass change of an ice particle due to the blowing
705 snow sublimation ~~due to higher moisture in the air, the deposition of water vapour at the surface increases, leading to only
a small change in the overall sublimation in winter. Though overall trends in the sublimation between~~ is given by the model
of Thorpe and Mason (1966) (Eq. (10)). Since the mass change depends on water vapour deficit and air temperature, accurate
prediction of these quantities is necessary to obtain reliable estimates of blowing snow sublimation. Table A1 shows that the
near-surface temperature is overpredicted for all three experiments, and all simulations have a slight positive temperature bias.
710 However, with the updates to the model, the bias in the model is improved from $1.61 \text{ }^\circ\text{C}$ for the NO-DRIFT case to 1.45
 $^\circ\text{C}$ for RpNew. RpNew also shows an improved temperature prediction with a lower bias of $0.3 \text{ }^\circ\text{C}$ compared to Rp3 ~~and~~.
The variability is modelled well, with an RMSE of 3°C , and a high $R^2 = 0.91$. The numbers show that RpNew predicts the
near-surface wind and temperature better than the other two experiments.

715 Appendix B: Blowing snow frequency

Figure B1 provides a colour-blind friendly version of ~~the~~ RpNew ~~appear to be the same, we observe a slight change in the
720 climatology of blowing~~ blowing snow frequency.

Appendix C: Difference between RpNew and Rp3

In Figure C1, we present the difference in some important variables between RpNew and Rp3 to quantify the magnitude of
720 change between the two versions. The blowing snow transport TR_{ds} (Fig. C1(b)) decreased somewhat over most of Antarctica

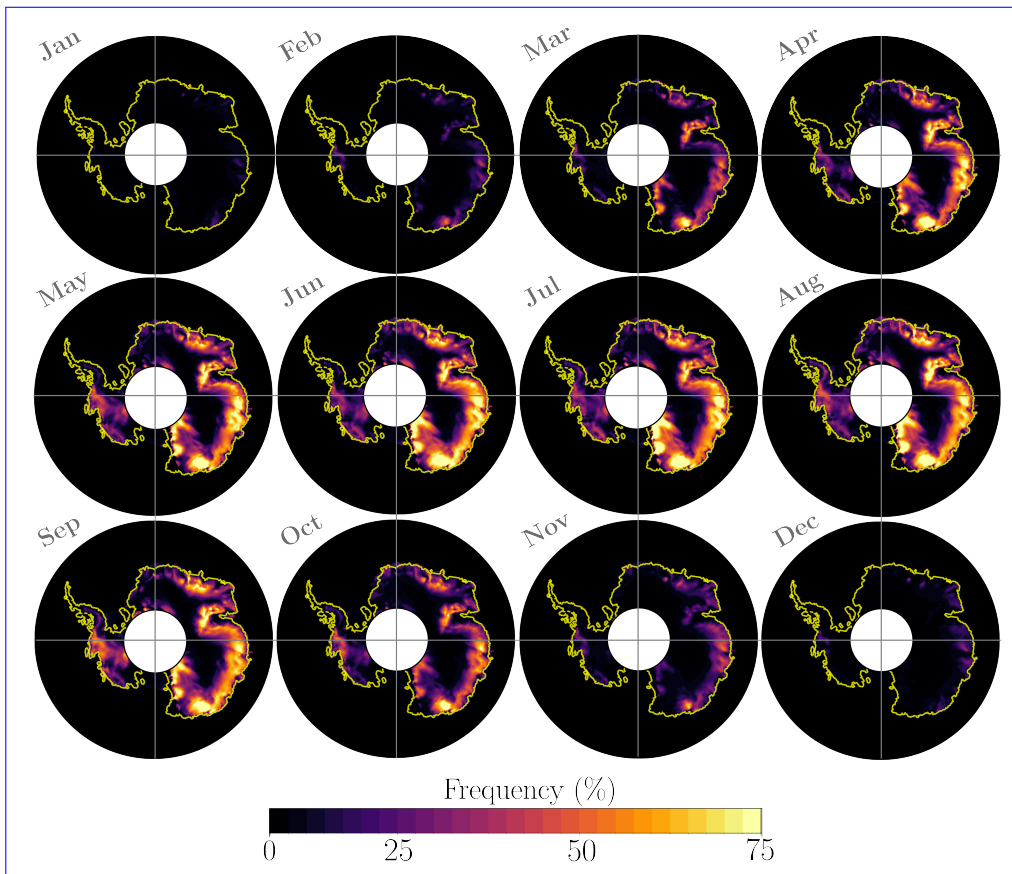


Figure B1. Blowing snow frequency visualised to provide a qualitative comparison with satellite measurements of Palm et al. (2018). Figures show the average blowing snow frequency from 2000 to 2012.

with significant but localised increases in transport along George V Land, Adélie Land, and Dronning Maud Land. At these locations, the blowing snow transport is increased by 2 - 3 times compared to Rp3 due to better modelling of snow particle distribution, which includes more particles with well-distributed ice particle radii and particle initialisation. As visualised in Figure C1(g) as an example, however, for most of Antarctica, most blowing snow events are reduced in intensity by the model updates. Only a few instances per year does the wind speed exceed the threshold for which the updated blowing snow model simulates higher blowing snow transport.

Conversely, for most of Antarctica, we observe higher blowing snow sublimation (Fig. C1(a)) due to the ability of RpNew to capture the peaks in blowing snow fluxes and the change in initialisation employed for the blowing snow model. This increase indicates the necessity of a direct two-way coupling of the atmosphere with the blowing snow model. In RpNew, the snow in the interior of Antarctica. In Rp3, the blowing snow sublimation was largely limited to the escarpment particles are lifted into the warmer and drier air of the upper part of the stable boundary layer. In Rp3, particles were not lifted that high - due to errors in the particle size distribution. The larger ice shelves are the only regions of Antarctica, with nearly zero where blowing snow

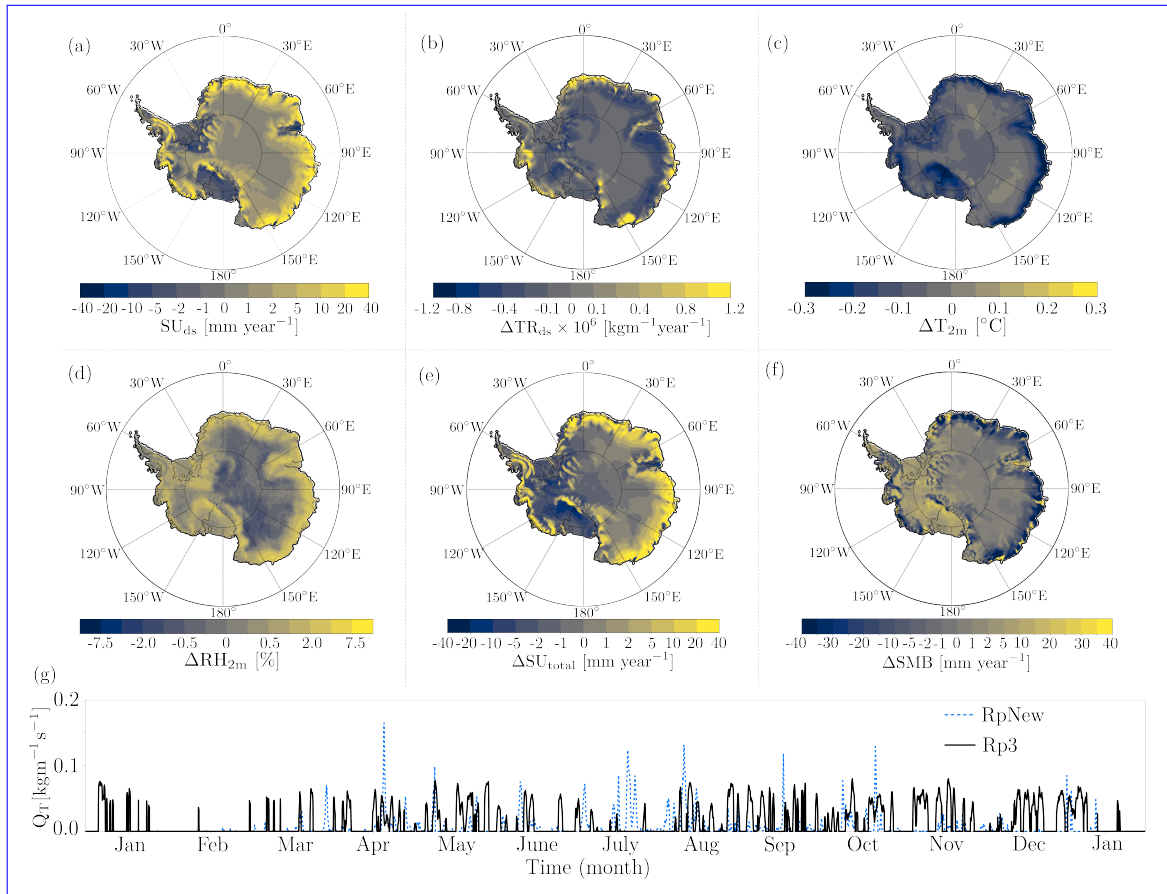


Figure C1. Yearly averaged (2000-2012) difference between RpNew and Rp3 quantities: (a) Blowing snow sublimation (mm yr^{-1}), (b) Blowing snow transport ($\text{kg m}^{-1}\text{yr}^{-1}$), (c) Near-surface temperature T_{2m} in $^{\circ}\text{C}$, (d) Relative humidity in percentage, (e) Total sublimation (mm yr^{-1}), and (f) SMB (mm yr^{-1}). SU_{ds} , SU_{total} , and SMB are in mm water equivalent. (g) Instantaneous drifting snow flux at an interior region of East Antarctica (71.1°S , 111.7°E).

sublimation ~~in the interior. RpNew results show that the results from~~ decreases. Here, the stable boundary layer is generally very thick (e.g. van den Broeke and Van Lipzig (2003), Fig. 10), inhibiting the blowing snow from reaching the warmer air above the surface layer.

735

Results show RpNew is slightly colder by 0.3–0.4 K (Fig. C1(c)) along the coastal areas when compared to Rp3 ~~different in both frequency and magnitude; the difference seems to be higher in the interior compared to the coastal Antarctica.~~ This results from a better coupling of blowing snow sublimation to the tendencies of temperature, which allows the removal of latent heat from upper vertical levels of Rp3. Compared to Rp3, RpNew has higher relative humidity (Fig. C1(d)) also, due to better coupling of blowing snow moisture tendencies, the change in moisture leads to an increase in the dew-point temperature of 2–4 K (not shown here) in the first few vertical layers of Rp3. Furthermore, the total sublimation is higher in RpNew (Fig. C1(e)) when

740

745 compared to Rp3. Along the coast, the difference is as high as $100 \text{ mm w.e. yr}^{-1}$. Overall, the averaged surface mass balance (Fig. C1(f)) is changed mostly along the coastal Antarctica with a reduction of approximately $30 - 40 \text{ mm w.e. yr}^{-1}$. Since there is an increase in the moisture availability, there is relatively higher precipitation over Ronne and Ross ice shelves with a corresponding increase in SMB of approximately $20 \text{ mm w.e. yr}^{-1}$.

750 In conclusion, ~~the updates introduced to the regional climate model RACMO in this study significantly improve the representation of blowing snow physics in RACMO. Blowing snow and surface sublimation are the major mass loss terms in the SMB of Antarctica, leading locally to a negative SMB, which results in the formation of blue ice areas. This study presents a step forward in modelling blowing snow in producing a physically sound and reliable estimate of the SMB of Antarctica.~~ changes introduced in RpNew greatly influence the overall sublimation pattern in Antarctica and moisture content in lower levels of the atmosphere. In the RpNew, blowing snow's impact is more regional than Rp3. However, the overall impact on SMB is limited, with a decrease in SMB on the Eastern Antarctic coast and a slight increase in SMB in Western Antarctica due to higher moisture content created by blowing snow sublimation.

755 Appendix D: Changes in integrated SMB between RpNew and Rp3

Table D1. Total ice sheet, including ice shelves, integrated SMB mean 2000–2012 values (Gt yr^{-1}) with interannual variability σ : total (snow and rain) precipitation (P_{tot}), total sublimation (SU_{tot}), surface sublimation (SU_s), blowing snow sublimation (SU_{ds}), blowing snow erosion (ER_{ds}), run-off (RU). Integrated surface mass balance is given by: $\text{SMB} = P_{\text{tot}} - SU_{\text{ds}} - SU_s - ER_{\text{ds}} - \text{RU}$.

	RpNew		Rp3		RpNew - Rp3
	mean	σ	mean	σ	mean (%change)
P_{tot}	2678	96	2655	98	+23 (0.9%)
SU_{tot}	234	10	186	6	+48 (26%)
SU_s	59	8	71	5	-12 (17%)
SU_{ds}	175	7	115	4	+60 (52%)
ER_{ds}	8	0.5	5	0.2	+3 (60%)
RU	7	3	7	3	0 (0%)
SMB	2428	97	2458	96	-30 (1.2%)

760 Table D1 presents the SMB and its components integrated over the whole ice sheet (including ice shelves) for the years 2000 – 2010 in Gt yr^{-1} along with their inter-annual variability. Compared to Rp3, RpNew has an increased precipitation of 23 Gt yr^{-1} caused by the higher moisture content in the atmosphere due to higher blowing snow sublimation. The total sublimation is increased by 48 Gt yr^{-1} with blowing snow sublimation being the major contributor. There is a slight decrease in surface sublimation (12 Gt yr^{-1}) as air in the boundary layer is saturated more efficiently with RpNew compared to Rp3, which causes a reduction in the potential for the surface sublimation. With higher blowing snow transport fluxes, we have a higher snow erosion

765 increase of 3 Gt yr⁻¹. This number remained small as snow erosion only influences the integrated SMB once the snow is blown off the ice sheet. Overall, the integrated SMB is reduced by 30 Gt yr⁻¹, due to a net increase in blowing snow sublimation. The change amounts to only a 1.2% decrease in SMB compared to Rp3. Since the SMB changes with the updates are minor and the SMB results from Rp2 have been previously evaluated against several in-situ and remote sensing observations, we refer to Noël et al. (2018); van Wessem et al. (2018) for the SMB evaluation. Though there is negligible change in the overall SMB, blowing snow sublimation is highly important to local SMB, especially in the escarpment areas in Eastern Antarctica.

770 *Acknowledgements.* We would like to thank Charles Amory for the discussion about observational dataset from site D47, East Antarctica. We would also like to thank Melchior van Wessem and Christiaan van Dalum for discussions about RACMO model development. This project has received funding from the European Union's Horizon 2020 research and innovation program under grant agreement no. 101003590 (PolarRES). We also acknowledge the ECMWF for archiving facilities and computational time on their supercomputers.

References

- Agosta, C., Amory, C., Kittel, C., Orsi, A., Favier, V., Gallée, H., van den Broeke, M. R., Lenaerts, J. T. M., van Wessem, M. J., van de Berg, W. J., et al.: Estimation of the Antarctic surface mass balance using the regional climate model MAR (1979–2015) and identification of dominant processes, *The Cryosphere*, 13, 281–296, <https://doi.org/10.5194/tc-13-281-2019>, 2019.
- 775
- Alduchov, O. A. and Eskridge, R. E.: Improved Magnus form approximation of saturation vapor pressure, *Journal of Applied Meteorology and Climatology*, 35, 601–609, [https://doi.org/https://doi.org/10.1175/1520-0450\(1996\)035%3C0601:IMFAOS%3E2.0.CO;2](https://doi.org/https://doi.org/10.1175/1520-0450(1996)035%3C0601:IMFAOS%3E2.0.CO;2), 1996.
- Amory, C.: Drifting-snow statistics from multiple-year autonomous measurements in Adélie Land, East Antarctica, *The Cryosphere*, 14, 1713–1725, <https://doi.org/10.5194/tc-14-1713-2020>, 2020.
- 780
- Amory, C., Trouvilliez, A., Gallée, H., Favier, V., Naaim-Bouvet, F., Genthon, C., Agosta, C., Piard, L., and Bellot, H.: Comparison between observed and simulated aeolian snow mass fluxes in Adélie Land, East Antarctica, *The Cryosphere*, 9, 1373–1383, <https://doi.org/10.5194/tc-9-1373-2015>, 2015.
- Amory, C., Gallée, H., Naaim-Bouvet, F., Favier, V., Vignon, E., Picard, G., Trouvilliez, A., Piard, L., Genthon, C., and Bellot, H.: Seasonal variations in drag coefficient over a sastrugi-covered snowfield in coastal East Antarctica, *Boundary-Layer Meteorology*, 164, 107–133, <https://doi.org/10.1007/s10546-017-0242-5>, 2017.
- 785
- Amory, C., Genthon, C., and Favier, V.: A drifting snow data set (2010–2018) from coastal Adélie Land, eastern Antarctica, Zenodo [data set], 10, <https://doi.org/10.5281/zenodo.3630496>, 2020a.
- Amory, C., Genthon, C., and Favier, V.: A drifting snow data set (2010–2018) from coastal Adélie Land, Eastern Antarctica, Data, <https://doi.org/10.5281/zenodo.3630497>, 2020b.
- 790
- Amory, C., Kittel, C., Toumelin, L. L., Agosta, C., Delhasse, A., Favier, A., and Fettweis, X.: Performance of MAR (v3.11) in simulating the drifting-snow climate and surface mass balance of Adélie Land, East Antarctica, *Geoscientific Model Development*, 14, 3487–3510, <https://doi.org/10.5194/gmd-14-3487-2021>, 2021.
- Barral, H., Genthon, C., Trouvilliez, A., Brun, C., and Amory, C.: Blowing snow in coastal Adélie Land, Antarctica: three atmospheric-moisture issues, *The Cryosphere*, 8, 1905–1919, <https://doi.org/10.5194/tc-8-1905-2014>, 2014.
- 795
- Bintanja, R.: The contribution of snowdrift sublimation to the surface mass balance of Antarctica, *Annals of Glaciology*, 27, 251–259, <https://doi.org/10.3189/1998AoG27-1-251-259>, 1998.
- Bintanja, R.: Snowdrift sublimation in a katabatic wind region of the Antarctic ice sheet, *Journal of Applied Meteorology and Climatology*, 40, 1952–1966, [https://doi.org/10.1175/1520-0450\(2001\)040<1952:SSIAKW>2.0.CO;2](https://doi.org/10.1175/1520-0450(2001)040<1952:SSIAKW>2.0.CO;2), 2001.
- 800
- Bromwich, D. H., Guo, Z., Bai, L., and Chen, Q.-S.: Modeled Antarctic precipitation. Part I: Spatial and temporal variability, *Journal of Climate*, 17, 427–447, [https://doi.org/https://doi.org/10.1175/1520-0442\(2004\)017%3C0427:MAPPIS%3E2.0.CO;2](https://doi.org/https://doi.org/10.1175/1520-0442(2004)017%3C0427:MAPPIS%3E2.0.CO;2), 2004.
- Budd, W. F.: The drifting of nonuniform snow particles, *Studies in Antarctic meteorology*, 9, 59–70, <https://doi.org/10.1029/AR009p0059>, 1966.
- CY45R1—Part IV, I. D.: Physical processes, IFS Documentation CY45R1, 2018.
- 805
- Déry, S. J. and Yau, M. K.: A bulk blowing snow model, *Boundary-Layer Meteorology*, 93, 237–251, <https://doi.org/10.1023/A:1002065615856>, 1999.
- Déry, S. J. and Yau, M. K.: Simulation of blowing snow in the Canadian Arctic using a double-moment model, *Boundary-Layer Meteorology*, 99, 297–316, <https://doi.org/10.1023/A:1018965008049>, 2001.

- Déry, S. J. and Yau, M. K.: Large-scale mass balance effects of blowing snow and surface sublimation, *Journal of Geophysical Research: Atmospheres*, 107, ACL–8, <https://doi.org/10.1029/2001JD001251>, 2002.
- 810 Déry, S. J., Taylor, P. A., and Xiao, J.: The thermodynamic effects of sublimating, blowing snow in the atmospheric boundary layer, *Boundary-Layer Meteorology*, 89, 251–283, <https://doi.org/10.1023/A:1001712111718>, 1998.
- ECMWF: IFS Documentation CY33R1 - Part IV: Physical Processes, 4, ECMWF, <https://doi.org/10.21957/8o7vwlbdr>, 2009.
- Ettema, J., van den Broeke, M. R., van Meijgaard, E., van de Berg, W. J., Box, J. E., and Steffen, K.: Climate of the Greenland ice sheet using a high-resolution climate model—Part 1: Evaluation, *The Cryosphere*, 4, 511–527, <https://doi.org/10.5194/tc-4-511-2010>, 2010.
- 815 Gallée, H., Guyomaréh, G., and Brun, E.: Impact of snow drift on the Antarctic ice sheet surface mass balance: possible sensitivity to snow-surface properties, *Boundary-Layer Meteorology*, 99, 1–19, <https://doi.org/10.1023/A:1018776422809>, 2001.
- Gelaro, R., McCarty, W., Suárez, M. J., Todling, R., Molod, A., Takacs, L., Randles, C. A., Darmenov, A., Bosilovich, M. G., Reichle, R., et al.: The modern-era retrospective analysis for research and applications, version 2 (MERRA-2), *Journal of climate*, 30, 5419–5454, <https://doi.org/10.1175/JCLI-D-16-0758.1>, 2017.
- 820 Gerber, F., Sharma, V., and Lehning, M.: Reproducibility dataset for CRYOWRF validation, <https://doi.org/http://dx.doi.org/10.16904/envidat.347>, 2022.
- Gerber, F., Sharma, V., and Lehning, M.: CRYOWRF—Model Evaluation and the Effect of Blowing Snow on the Antarctic Surface Mass Balance, *Journal of Geophysical Research: Atmospheres*, 128, e2022JD037 744, <https://doi.org/10.1029/2022JD037744>, 2023.
- 825 Greuell, W. and Konzelmann, T.: Numerical modelling of the energy balance and the englacial temperature of the Greenland Ice Sheet. Calculations for the ETH-Camp location (West Greenland, 1155 m asl), *Global and Planetary change*, 9, 91–114, [https://doi.org/10.1016/0921-8181\(94\)90010-8](https://doi.org/10.1016/0921-8181(94)90010-8), 1994.
- Hersbach, H., Bell, B., Berrisford, P., Hirahara, S., Horányi, A., Muñoz-Sabater, J., Nicolas, J., Peubey, C., Radu, R., Schepers, D., et al.: The ERA5 global reanalysis, *Quarterly Journal of the Royal Meteorological Society*, 146, 1999–2049, <https://doi.org/10.1002/qj.3803>, 2020.
- 830 King, J. C., Anderson, P. S., Smith, M. C., and Mobbs, S. D.: The surface energy and mass balance at Halley, Antarctica during winter, *Journal of Geophysical Research: Atmospheres*, 101, 19 119–19 128, <https://doi.org/10.1029/96JD01714>, 1996.
- King, J. C., Anderson, P. S., and Mann, G. W.: The seasonal cycle of sublimation at Halley, Antarctica, *Journal of Glaciology*, 47, 1–8, <https://doi.org/10.3189/172756501781832548>, 2001.
- Kodama, Y., Wendler, G., and Gosink, J.: The effect of blowing snow on katabatic winds in Antarctica, *Annals of Glaciology*, 6, 59–62, <https://doi.org/10.3189/1985AoG6-1-59-62>, 1985.
- 835 Kuipers Munneke, P., Van den Broeke, M., Lenaerts, J., Flanner, M., Gardner, A., and Van de Berg, W.: A new albedo parameterization for use in climate models over the Antarctic ice sheet, *Journal of Geophysical Research: Atmospheres*, 116, <https://doi.org/10.1029/2010JD015113>, 2011.
- Lenaerts, J. T. M. and van den Broeke, M. R.: Modeling drifting snow in Antarctica with a regional climate model: 2. Results, *Journal of Geophysical Research: Atmospheres*, 117, <https://doi.org/10.1029/2010JD015419>, 2012.
- 840 Lenaerts, J. T. M., van den Broeke, M. R., Déry, S. J., van Meijgaard, E., van de Berg, W. J., Palm, S. P., and Rodrigo, J. S.: Modeling drifting snow in Antarctica with a regional climate model: 1. Methods and model evaluation, *Journal of Geophysical Research: Atmospheres*, 117, <https://doi.org/10.1029/2011JD016145>, 2012.
- Lenaerts, J. T. M., Smeets, C. J. P. P., Nishimura, K., Eijkelboom, M., Boot, W., van den Broeke, M. R., and van de Berg, W. J.: Drifting snow measurements on the Greenland Ice Sheet and their application for model evaluation, *The Cryosphere*, 8, 801–814, <https://doi.org/10.5194/tc-8-801-2014>, 2014.
- 845

- Libois, Q., Picard, G., France, J. L., Arnaud, L., Dumont, M., Carmagnola, C. M., and King, M. D.: Influence of grain shape on light penetration in snow, *The Cryosphere*, 7, 1803–1818, <https://doi.org/10.5194/tc-7-1803-2013>, 2013.
- 850 Mottram, R., Hansen, N., Kittel, C., van Wessem, J. M., Agosta, C., Amory, C., Boberg, F., van de Berg, W. J., Fettweis, X., Gossart, A., et al.: What is the surface mass balance of Antarctica? An intercomparison of regional climate model estimates, *The Cryosphere*, 15, 3751–3784, <https://doi.org/10.5194/tc-15-3751-2021>, 2021.
- Noël, B., van de Berg, W. J., van Wessem, M. J., van Meijgaard, E., van As, D., Lenaerts, J., Lhermitte, S., Munneke, P. K., Smeets, C. J. P., van Ulft, L. H., et al.: Modelling the climate and surface mass balance of polar ice sheets using RACMO2–Part 1: Greenland (1958–2016), *The Cryosphere*, 12, 811–831, <https://doi.org/10.5194/tc-12-811-2018>, 2018.
- 855 Palm, S. P., Yang, Y., Spinhirne, J. D., and Marshak, A.: Satellite remote sensing of blowing snow properties over Antarctica, *Journal of Geophysical Research: Atmospheres*, 116, <https://doi.org/10.1029/2011JD015828>, 2011.
- Palm, S. P., Kayetha, V., Yang, Y., and Pauly, R.: Blowing snow sublimation and transport over Antarctica from 11 years of CALIPSO observations, *The Cryosphere*, 11, 2555–2569, <https://doi.org/10.5194/tc-11-2555-2017>, 2017.
- Palm, S. P., Kayetha, V., and Yang, Y.: Toward a satellite-derived climatology of blowing snow over Antarctica, *Journal of Geophysical Research: Atmospheres*, 123, 10–301, <https://doi.org/10.1029/2018JD028632>, 2018.
- 860 Pomeroy, J. W.: A process-based model of snow drifting, *Annals of Glaciology*, 13, 237–240, <https://doi.org/10.3189/S0260305500007965>, 1989.
- Pomeroy, J. W. and Male, D. H.: Steady-state suspension of snow, *Journal of hydrology*, 136, 275–301, [https://doi.org/10.1016/0022-1694\(92\)90015-N](https://doi.org/10.1016/0022-1694(92)90015-N), 1992.
- 865 Radok, U.: Snow drift, *Journal of Glaciology*, 19, 123–139, <https://doi.org/10.3189/S0022143000215591>, 1977.
- Scambos, T. A., Frezzotti, M., Haran, T., Bohlander, J., Lenaerts, J., Van Den Broeke, M., Jezek, K., Long, D., Urbini, S., Farness, K., et al.: Extent of low-accumulation ‘wind glaze’ areas on the East Antarctic plateau: implications for continental ice mass balance, *Journal of glaciology*, 58, 633–647, <https://doi.org/10.3189/2012JoG11J232>, 2012.
- Scarchilli, C., Frezzotti, M., Grigioni, P., Silvestri, L. D., Agnoletto, L., and Dolci, S.: Extraordinary blowing snow transport events in East Antarctica, *Climate Dynamics*, 34, 1195–1206, <https://doi.org/10.1007/s00382-009-0601-0>, 2010.
- 870 Schmidt, R. A.: Sublimation of wind-transported snow: a model, vol. 90, Rocky Mountain Forest and Range Experiment Station, Forest Service, US . . . , 1972.
- Schmidt, R. A.: Vertical profiles of wind speed, snow concentration, and humidity in blowing snow, *Boundary-Layer Meteorology*, 23, 223–246, <https://doi.org/10.1007/BF00123299>, 1982.
- 875 Serreze, M. C. and Barry, R. G.: *The Arctic climate system*, Cambridge University Press, 2005.
- Thiery, W., Gorodetskaya, I. V., Bintanja, R., van Lipzig, N. P. M., van den Broeke, M. R., Reijmer, C. H., and Munneke, P. K.: Surface and snowdrift sublimation at Princess Elisabeth station, East Antarctica, *The Cryosphere*, 6, 841–857, <https://doi.org/10.5194/tc-6-841-2012>, 2012.
- Thorpe, A. and Mason, B.: The evaporation of ice spheres and ice crystals, *British Journal of Applied Physics*, 17, 541, <https://doi.org/10.1088/0508-3443/17/4/316>, 1966.
- 880 Toumelin, L. L., Amory, C., Favier, V., Kittel, C., Hofer, S., Fettweis, X., Gallée, H., and Kayetha, V.: Sensitivity of the surface energy budget to drifting snow as simulated by MAR in coastal Adelie Land, Antarctica, *The Cryosphere*, 15, 3595–3614, <https://doi.org/10.5194/tc-15-3595-2021>, 2021.

- Undén, P., Rontu, L., Jarvinen, H., Lynch, P., Sánchez, F. J. C., Cats, G., Cuxart, J., Eerola, K., Fortelius, C., García-Moya, J. A., et al.:
885 HIRLAM-5 scientific documentation, <http://hdl.handle.net/20.500.11765/6323>, 2002.
- van Dalum, C. T., van de Berg, W. J., Libois, Q., Picard, G., and van den Broeke, M. R.: A module to convert spectral to narrowband snow
albedo for use in climate models: SNOWBAL v1. 2, *Geoscientific Model Development*, 12, 5157–5175, <https://doi.org/10.5194/gmd-12-5157-2019>, 2019.
- van Dalum, C. T., van de Berg, W. J., and van den Broeke, M. R.: Sensitivity of Antarctic surface climate to a new spectral snow albedo and
890 radiative transfer scheme in RACMO2.3p3, *The Cryosphere*, 16, 1071–1089, <https://doi.org/10.5194/tc-16-1071-2022>, 2022.
- van den Broeke, M. and Bintanja, R.: The interaction of katabatic winds and the formation of blue-ice areas in East Antarctica, *Journal of
Glaciology*, 41, 395–407, <https://doi.org/10.3189/S0022143000016269>, 1995.
- van den Broeke, M. and Van Lipzig, N.: Factors controlling the near-surface wind field in Antarctica, *Monthly Weather Review*, 131, 733–
743, 2003.
- 895 van den Broeke, M. R., Reijmer, C. H., and van de Wal, R. S. W.: A study of the surface mass balance in Dronning Maud Land, Antarctica,
using automatic weather stations, *Journal of Glaciology*, 50, 565–582, <https://doi.org/10.3189/172756504781829756>, 2004.
- van Meijgaard, E., van Ulft, L., Lenderink, G., de Roode, S. R., Wipfler, E. L., Boers, R., and van Timmermans, R. M. A.: Refinement and
application of a regional atmospheric model for climate scenario calculations of Western Europe, KVR 054/12, KvR, <https://library.wur.nl/WebQuery/wurpubs/427097>, 2012.
- 900 van Wessem, J. M., Ligtenberg, S. R. M., Reijmer, C. H., van de Berg, W. J., van den Broeke, M. R., Barrand, N. E., Thomas, E. R., Turner,
J., Wuite, J., Scambos, T. A., et al.: The modelled surface mass balance of the Antarctic Peninsula at 5.5 km horizontal resolution, *The
Cryosphere*, 10, 271–285, <https://doi.org/10.5194/tc-10-271-2016>, 2016.
- van Wessem, M. J., Reijmer, C. H., van de Berg, W. J., van den Broeke, M. R., Cook, A. J., van Ulft, L. H., and van Meijgaard, E.: Temperature
and wind climate of the Antarctic Peninsula as simulated by a high-resolution regional atmospheric climate model, *Journal of Climate*,
905 28, 7306–7326, <https://doi.org/10.1175/JCLI-D-15-0060.1>, 2015.
- van Wessem, M. J., van de Berg, W. J., Noël, P. Y. B., van Meijgaard, E., Amory, C., Birnbaum, G., Jakobs, C. L., Krüger, K., Lenaerts,
J. T. M., Lhermitte, S., et al.: Modelling the climate and surface mass balance of polar ice sheets using RACMO2–Part 2: Antarctica
(1979–2016), *The Cryosphere*, 12, 1479–1498, <https://doi.org/10.5194/tc-12-1479-2018>, 2018.
- Vinokur, M.: On one-dimensional stretching functions for finite-difference calculations, *Journal of Computational Physics*, 50, 215–234,
910 [https://doi.org/https://doi.org/10.1016/0021-9991\(83\)90065-7](https://doi.org/https://doi.org/10.1016/0021-9991(83)90065-7), 1983.